JOURNAL OF GEOPHYSICAL RESEARCH, VOL. 106, NO. A11, PAGES 25,141–25,163, NOVEMBER 1, 2001

Coronal mass ejections, magnetic flux ropes, and solar magnetism

B. C. Low

High Altitude Observatory, National Center for Atmospheric Research, Boulder, Colorado

Abstract. This review on coronal mass ejections (CMEs) treats hydromagnetic issues posed by observations, in order to relate CMEs to flares and prominence eruptions and to consider the roles these processes play in the evolution of the solar corona in the course of an 11-year cycle. This global view of the corona, proposed in varying degrees of completeness by the author, physically connects the corona to the photosphere and the dynamo in the solar interior. This view is synthesized afresh starting with CME phenomenology, in order to include some new insights and to arrive at definite statements on the hydromagnetic nature of CMEs. The synthesis shows that each CME culminates a long, coherent physical process involving magnetic-flux emergence; flares and magnetic reconnection; creation of long-lived, large-scale coronal structures; conservation of magnetic helicity; and failure of confinement of magnetic flux ropes in the open atmosphere. Each CME contributes a systematic permanent change to the coronal magnetic field. In this view the cumulative changes brought by all the CMEs in the course of a solar cycle have fundamental implications for the magnetic-flux budgets of the photosphere and the corona.

1. Introduction

The wealth of solar coronal phenomena that we call solar activity should be viewed beyond their individual occurrences. Collectively, they are the dynamical response of the solar corona to the variable solar magnetic field. In each 11-year magnetic cycle, magnetic flux is injected from the solar interior into the corona. The injection is not a completely chaotic process but one that systematically reverses the global magnetic polarity within a few years from the first appearance of sunspot belts belonging to the new cycle. The million-degree corona is practically a perfect electrical conductor. The mixing of old and new magnetic fluxes in this hydromagnetic atmosphere involves a whole gamut of plasma processes, producing relatively long lived structures such as quiescent prominences and sunspots, as well as highly time dependent phenomena such as flares and coronal mass ejections (CMEs). In these broad terms the physical picture is widely accepted.

To go deeper in our understanding, we need insights that can relate what we currently know from observations to ideas based on physical principles. Such insights cannot be had simply on demand, but must come from answering good physical questions posed within a relatively complete observational knowledge. The discovery of CMEs in the 1970s followed by observational studies of this phenomenon brought about a completeness insofar as coronal phenomenology is concerned [*Gosling et al.*, 1974; *MacQueen*, 1980; *MacQueen et al.*, 2001; *Fisher*, 1984; *Howard et al.*, 1985, 1997; *Hundhausen*, 1987, 1993, 1999; *Hundhausen, Burkepile, and St. Cyr*, 1994; *Low*, 1990, 1996; *Kahler*, 1992; *Burkepile and St. Cyr*, 1993; *St. Cyr et al.*, 1999; *St. Cyr et al.*, 2000; *Crooker et al.*, 1997; *Dere et al.*, 1999; *Forbes*, 2000]. With this development it has become possible to synthesize a hydromagnetic description of the corona capable of relating diverse phenomena into a meaningful whole [*Low*, 1994, 1996, 1997, 1999a].

In the following sections we synthesize this description afresh, on the basis of an extensive but not exhaustive survey of literature. We start with CME observations and theory (section 2), work through the physical questions posed by helmet streamers (section 3), the relationship between flares and long lived structures (section 4), and the connection between CMEs and the solar dynamo (section 5). Our conclusions are given in section 6. We will give a definite statement on the hydromagnetic nature of CMEs. Our synthesis makes a compelling case for the formation of magnetic flux ropes in the corona as the origin of the CME phenomenon. If this description is valid, we will have succeeded in bridging phenomenology to hydromagnetic principles. If this description is not valid or requires modification, a possibility facing any theory as an ongoing development, its rejection or revision will be instructive.

Paper number 2000JA004015.
0148-0227/01/2000JA004015$09.00

2. Coronal Mass Ejections

A good starting point for our synthesis is the average mass loss contributed by CMEs. The rate of occurrence of CMEs is one to three events a day, and the mass of each CME is about 10^{15-16} g [*Howard et al.*, 1985; *Hundhausen*, 1999]. These observations imply a mass-loss rate of about 10^{11} $g\ s^{-1}$. Individual CMEs are significant perturbations in the solar wind and they may be a driver of "space weather" at Earth orbit [*Fox et al.*, 1998]. However, they contribute to an average coronal mass-loss rate smaller than or about 10% of the mass-loss rate in the steady solar wind [*MacQueen*, 1980; *Webb and Howard*, 1994]. The solar wind is clearly the more important mass-loss process in the balance of energy and mass in the large-scale corona.

2.1. Magnetic Effects of CMEs

The significance of CMEs is their magnetic effects on the corona as a hydromagnetic atmosphere [*Low*, 1994]. In addition to energy and mass balance, the electrically highly conducting corona must also process its magnetic fluxes, the newly emerged and the old. Until the discovery of CMEs in the 1970s, the view was that flares are localized small-scale eruptions due to magnetic flux emergence, whereas the large-scale corona evolved gradually on solar-cycle timescales between the two characteristic global forms shown in Figure 1. This view changed radically after CMEs became known. We now accept that the slow evolution of the large-scale corona is punctuated daily by one to three reconfigurations associated with CMEs. This realization raises the question posed by *Low* [1997] of whether each CME influences the coronal magnetic field in a permanent way.

To appreciate the question, consider the shearing of a coronal magnetic field by the displacement of its magnetic foot points in the photosphere. Suppose such a process proceeds with no transport of magnetic flux across the photosphere, either downward transport from above or upward transport from below. Let this process reach the point of an eruption which opens up the coronal magnetic field to release the magnetic shear created, as demonstrated in many models [e.g., *Low*, 1977, 1986; *Steinolfson*, 1991; *Wolfson and Low*, 1992; *Wolfson*, 1993; *Mikic and Linker*, 1994; *Linker and Mikic*, 1995; *Aly*, 1995; *Antiochos et al.*, 1999]. This process would have taken the magnetic field from an unsheared, initial state back to an unsheared state at the end of it. The amount of magnetic flux of a given sign threading across the coronal base is unchanged. Therefore the whole process from slow energy buildup to rapid energy release would have produced no permanent change to the coronal magnetic environment.

On the other hand, if two additional effects take place, then the process can produce a permanent magnetic change. The two effects are (1) magnetic flux emergence and (2) the bodily transport of a flux system into the corona [*Lites et al.*, 1995; *Feynman and Martin*, 1995; *Low*, 1997; *Luhmann et al.*, 1998]. Once in the corona, such a flux system may at first persist in some metastable state and then be further transported out into interplanetary space with a CME. From this point of view, CMEs may be the hydromagnetic process that enables the corona to rid itself of its old magnetic field for replacement with a new global field of the opposite polarity. To establish this point of view on a physical basis is the motivation of this review.

2.2. CME Energetics and Dynamics

CME speeds measured in terms of the speeds of such features as the CME front edge fall in a broad range from about 20 $km\ s^{-1}$ to 2×10^3 $km\ s^{-1}$ [*Gosling et al.*, 1976; *Howard et al.*, 1985; *Hundhausen et al.*, 1994; *St. Cyr et al.*, 1999, 2000]. The coronagraphs of the Solar Maximum Mission (SMM) and the Solar and Heliospheric Observatory (SOHO) show median CME speeds of about 450 $km\ s^{-1}$. Sound speeds at million-degree temperatures are about 100 $km\ s^{-1}$, and coronal Alfven speeds can be estimated to be about 10^3 $km\ s^{-1}$. The gravitational escape speed near the base of the corona where the CMEs originate is about 550 $km\ s^{-1}$. So CMEs tend to be supersonic, but sub-Alfvenic in the corona, with implications for the hydromagnetic shocks driven ahead of the CMEs [*Sheeley et al.*, 1985; *Hundhausen et al.*, 1987; *Hu et al.*, 1990; *Steinolfson and Hundhausen*, 1990; *De Sterck et al.*, 1998].

Most CMEs show constant speeds or constant accelerations at speeds below the gravitational escape speed, even for speeds at the extreme low end of the observed range of speeds [*Low et al.*, 1982; *Fisher and Garcia*, 1984; *Illing and Hundhausen*, 1985; *Srivastava et al.*, 1999]. Clearly, gravitational force is important for most CMEs, as evidenced by the fact that the median CME speed is comparable to the escape speed. The relative absence of deceleration suggests that CMEs are generally driven by magnetic and pressure forces that either cancel or overwhelm gravity once CMEs are in motion.

Taking a large CME mass of 10^{16} g, the median-speed CME has a kinetic energy of 10^{31} $ergs$. To lift this mass out of the corona requires work done against gravity given by the kinetic energy associated with the escape speed, 1.5×10^{31} $ergs$, which is slightly larger than the CME kinetic energy. This gravitational work is fixed by the CME mass of 10^{16} g, independent of its outward speed. The CME energy, kinetic energy plus gravitational work, comes from coronal magnetic fields [*Hundhausen*, 1987, 1999; *Low*, 1990; *Antiochos et al.*, 1999; *Forbes*, 2000]. For CMEs moving at below the median speed, the magnetic field puts more energy into doing work against gravity than into the CME motion. For similar-mass CMEs moving at the high end of the speed range, say, the relatively rare events of CME speeds at 10^3 $km\ s^{-1}$ [*St. Cyr et al.*, 1999], the kinetic energy of the CME is about 5×10^{31} $ergs$, a factor of three larger than the gravitational work.

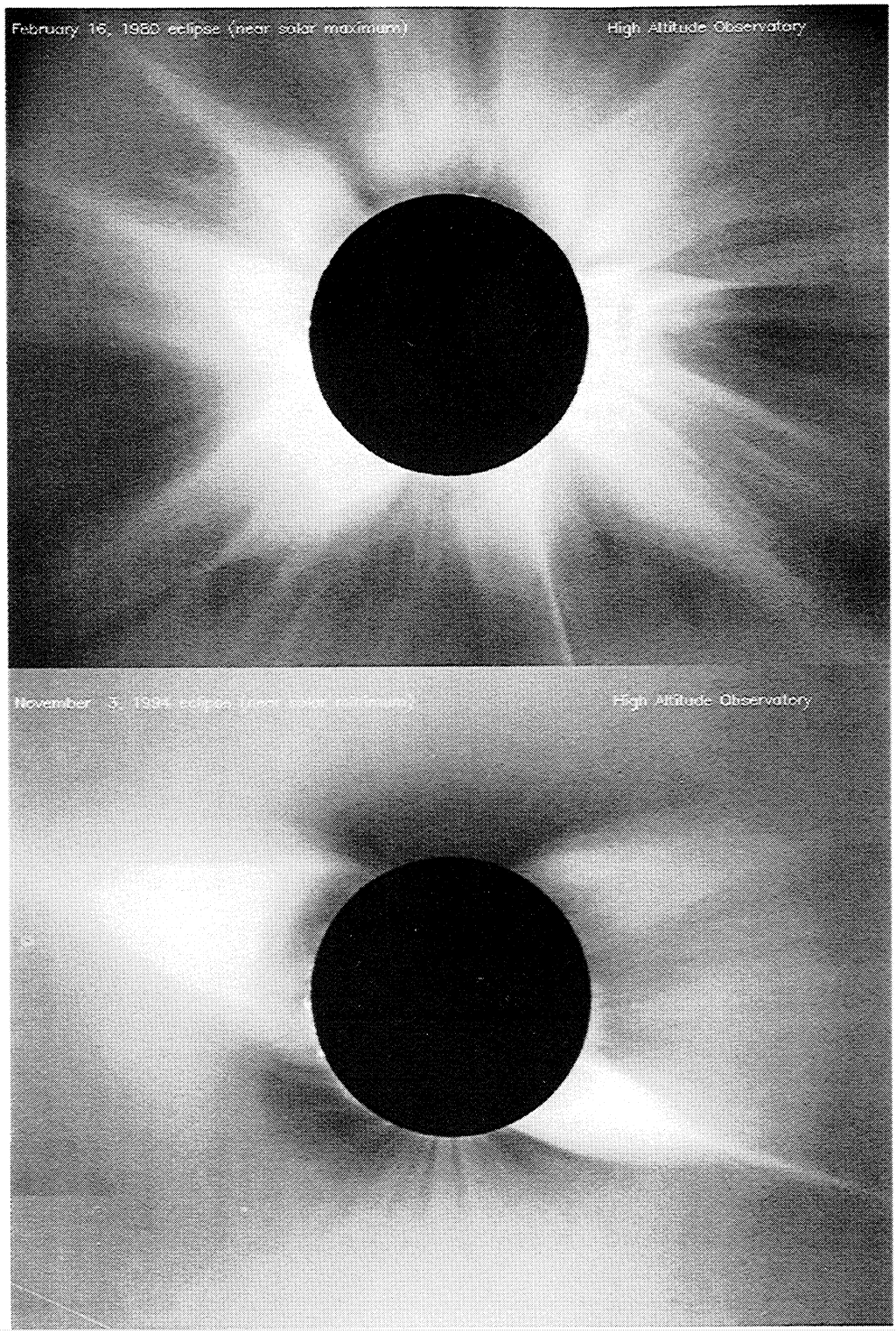

Figure 1. Two characteristic global configurations of the corona. The total solar eclipse of February 16, 1980 in the upper panel occurred at maximum solar activity, displaying coronal helmet streamers all around the Sun. The magnetic field of the Sun was undergoing global field reversal at this time, with a negligible dipole moment. The spherically radial form of the corona evolved rapidly within a year to a more "dipolar" form when the field reversal reached completion with the establishment of a dipole moment opposite in sign to that in the previous solar cycle. The total eclipse of November 3, 1994, in the lower panel, occurred at minimum solar activity, displaying only a main belt of helmet streamers encircling the Sun and meandering closer to the equator than to the solar poles. The two eclipse photographs are taken from the High Altitude Observatory's archive of coronal data.

An essential aspect of CME dynamics is illustrated by the hydromagnetic scaling laws governing the spherical, homologous expansion of a magnetized plasma in a r^{-2} gravitational field. If R is the increasing radius of the expanding sphere, the plasma mean density would scale as $\rho_{\text{mean}} \propto R^{-3}$ and the embedded magnetic field intensity would scale as $B_{\text{mean}} \propto R^{-2}$ to conserve mass and magnetic fluxes, respectively. This implies that the mean gravitational potential energy density in the expanding sphere would scale as $\rho_{\text{mean}} R^{-1} \propto R^{-4}$. If the assumed homologous expansion is to be driven by the magnetic field and plasma pressure, these drivers must maintain their energy densities to exceed or be comparable to the mean gravitational potential energy density R^{-4} during the expansion. This condition is met in the case of magnetic energy whose mean density scales as $B^2_{\text{mean}} \propto R^{-4}$, the same power law as for the mean gravitational potential energy density. For a polytropic plasma of index γ, the internal energy density of the plasma scales as $p_{\text{mean}} \propto \rho^{\gamma}_{\text{mean}} \propto R^{-3\gamma}$. So for the plasma pressure to keep up with doing work against gravity, $\gamma \leq 4/3$ is required.

These scaling laws demonstrate that the magnetic field is naturally capable of driving mass out of a gravitational potential well. Plasma pressure is also needed [*Low*, 1993a]. We should bear in mind that the Lorentz force is everywhere acting perpendicular to the magnetic field. This means that pressure force must act against gravity in the direction parallel to the magnetic field, if a coherent, everywhere outward expansion of a CME structure is to be sustained at expansion speeds at or below the gravitational escape speed [*Low*, 1984].

The corona, composed mainly of ionized hydrogen, has an adiabatic index of 5/3. By the above scaling laws, the adiabatic thermal energy is inadequate for driving mass out of the corona. Coronal plasma is, of course, not adiabatic but is subject to heating by thermal conduction and direct energy addition via mechanisms still being debated in the research community [*Parker*, 1994]. If we model heated coronal plasma mathematically as a polytropic gas with an index γ artificially set smaller than 5/3, the feature of heat addition is then represented qualitatively by the pressure behavior $p \propto \rho^{\gamma}$ in an expansive flow. The decrease of pressure with density would proceed less rapidly than in the case of pure adiabatic expansion [*Parker*, 1963; *Hundhausen*, 1972]. In this mathematical approximation we need $\gamma \leq 4/3$ to sustain a homologous expansion.

We are dealing with CMEs as time-dependent expansive flows. It is instructive to contrast the above restriction on the polytropic index with a similar restriction in the theory of the polytropic, steady state solar wind [*Parker*, 1963]. In the Parker theory the existence of the solar wind requires $\gamma \leq 3/2$ to ensure that the steady outflow has sufficient polytropic internal energy to overcome gravity. The steady wind also reminds us that the corona is an open system, so that it is not the internal energy density $p/(\gamma - 1)$ but the larger enthalpy density $\gamma p/(\gamma - 1)$ that is the source of energy. This is because the expulsion of each parcel of gas is aided by the work done by the pressure of the gas moving beneath it. Approximately half the available enthalpy goes into gravitational work, and the other half goes into the terminal kinetic energy of the wind [*Parker*, 1963]. The comparable kinetic and gravitational potential energies of most CMEs suggest that a similar partition of energy governs the time-dependent CME acceleration.

To treat the expulsion of a CME quantitatively, an ideal, polytropic, hydromagnetic description in terms of a single fluid is appropriate. The governing equations are

$$\rho \left[\frac{\partial \mathbf{v}}{\partial t} + (\mathbf{v} \cdot \nabla) \mathbf{v} \right] = \frac{1}{4\pi} (\nabla \times \mathbf{B}) \times \mathbf{B} - \nabla p - \frac{GM_{\odot}}{r^2} \hat{r}, \tag{1}$$

$$\frac{\partial \mathbf{B}}{\partial t} = \nabla \times (\mathbf{v} \times \mathbf{B}), \tag{2}$$

$$\frac{\partial \rho}{\partial t} + \nabla \cdot (\rho \mathbf{v}) = 0, \tag{3}$$

$$\frac{\partial}{\partial t} \left(p \rho^{-\gamma} \right) + \mathbf{v} \cdot \nabla \left(p \rho^{-\gamma} \right) = 0, \tag{4}$$

where $\mathbf{B}$, $\mathbf{v}$, p, and ρ are the magnetic field, velocity field, pressure, and density, respectively. Note that momentum equation (1) includes solar gravity in standard notation. A numerical treatment is generally necessary, especially for three-dimensional systems.

The identical homologous scalings of magnetic, polytropic internal and gravitational potential energy densities in the case of $\gamma = 4/3$ manifest in the existence of self-similar, time-dependent solutions to (1)–(4) for this particular polytrope [*Low*, 1982, 1984]. There is no physical reason for $\gamma = 4/3$ to especially apply to the corona. These self-similar solutions are useful as direct hydromagnetic demonstrations of CME motion without the need to undertake complex numerical simulation. The solutions describe the main flows of white-light CMEs, as distinct from the wave front or shock wave traveling ahead of a CME and propagating into the yet undisturbed coronal atmosphere. Explicit solutions obtained have shown how the time-dependent transport of plasma, polytropic internal energy, and magnetic field is able to maintain the forces required to drive a coherent large-scale structure out of the corona. The free parameters of these solutions allow for the expulsion to proceed at speeds in a broad range, with or without acceleration, from well below sound and gravitational escape speeds to supersonic and super-Alfvenic speeds.

In particular, the three forces may even be in exact equilibrium, i.e., with zero net force within the CME structure, during the expansion. In this instructive special case, each parcel of plasma moves by its inertia at

a constant speed [*Low*, 1984]. At any instant, the constant speeds of different parts of the CME give a velocity distribution which has a linear dependence on the Sun-centered radial distance. These properties are qualitatively characteristic of CMEs, although the quantitative forms of the self-similar hydromagnetic flows do not agree in detail with observed CME velocity distributions [*Illing*, 1984; *Low and Hundhausen*, 1987; *Athay et al.*, 1987].

2.3. CMEs With Three-part Structures

There is a major class of CMEs characterized by a three-part structure when observed in white light [*Fisher and Poland*, 1981; *Low et al.*, 1982; *Illing and Hundhausen*, 1985, 1986; *Howard et al.*, 1985; *Hundhausen*, 1987, 1999; *Dere et al.*, 1999]. Plate 1 shows two good examples of CMEs displaying a bright, high-density front moving ahead of a dark, low-density cavity, within which a bright, relatively high density core is found. Many CMEs show low-density cavities without a bright core. These cavities may in fact contain no high-density core. Alternatively, a high-density core in a cavity may become insignificant in Thomson-scattered light when observed from some fortuitous perspective [*Gibson and Low*, 1998, 2000].

In the SMM coronagraph data set, CMEs displaying the high-density front and trailing cavity, with or without the core, make up about 47% of the CMEs observed [*Burkepile and St. Cyr*, 1993]. In the first 2 years of operation, the Large-Angle and Spectrometric Coronagraphs (LASCO) reported 25–50% of the observed CMEs to be of this class [*Dere et al.*, 1999]. Although this percentage varies from one data set to another, the important point for the purpose of this review is that this kind of CME is common and forms a distinct, identifiable class (see the discussion by *Hundhausen* [1999]). Its characteristic structure holds the clue to the hydromagnetic nature of CMEs. We shall hereinafter focus our attention on these CMEs, referring to them generally as the three-part CMEs.

Observations suggest that three-part CMEs originate from the eruption of a coronal helmet streamer; see the August 18, 1980 CME event in Plate 1. Where observations are complete and of good quality, the helmet prior to eruption into a CME also shows a corresponding three-part structure: dense helmet dome, dark cavity at the helmet base, and a quiescent prominence inside the cavity [*Tandberg-Hanssen*, 1995; *Low and Hundhausen*, 1995]. Especially in the case of the lower-speed CMEs, the eruption is reasonably interpreted to be one that preserves the coherence of the three-part structure of the helmet. Excellent examples of the three-part helmet, in the quiescent state, can be seen in the photographs of the March 18, 1988 and July 11, 1991, total eclipses published by *Sime et al.* [1988] and *Sime and Streete* [1993].

Outside of quiescent prominences, the magnetic field in the corona cannot be readily measured; this should always be kept in mind. However, interpretation of observations seems persuasive that CMEs originate from closed magnetic configurations which are forced open in the course of a CME expulsion [*Hundhausen*, 1987, 1999]. CMEs appear to behave differently depending on whether the expulsions occur over an active region or away from an active region.

The latter is exemplified by the helmet-streamer belts over polar crown filaments, associated with old active regions [*Tandberg-Hanssen*, 1995]. The polarity inversion lines under these helmet-streamer belts are long, with lengths of 1-3 $R_\odot$. CMEs originating from active regions, of course, involve the more complex geometry of the intense magnetic fields of such regions [*Webb et al.*, 1997; *Antiochos*, 1998; *Antiochos et al.*, 1999]. These CMEs are characterized by a high constant speed already acquired low in the corona [*MacQueen and Fisher*, 1983; *St. Cyr et al.*, 1999; *Dere et al.*, 1999; *Sheeley, Jr. et al.*, 1999]. In contrast, the prominence-associated CMEs erupting away from active regions tend to start with low speeds which detectably increase as the CMEs travel through the corona.

The three-part structure can be found in CMEs independent of whether they are associated with active regions. In other words, separate from the variations in their physical circumstances and detailed behaviors, these CMEs share a common magnetic topology associated with their three-part structure.

The $\gamma = 4/3$ self-similar, time-dependent solutions allow for full variations in three-dimensional space. This mathematical feature was exploited by *Gibson and Low* [1998, 2000] in an exact MHD model for the three-part structure of CMEs in terms of a specific twisted magnetic field in realistic geometry. CMEs are usually observed with a white-light coronagraph which is ideal for observing CMEs leaving from a solar limb. The nature of Thomson scattering renders CMEs leaving from the disk-center difficult for coronagraph detection except where the CME is unusually massive and the instrument is adequately sensitive [*Howard et al.*, 1982; *Plunkett et al.*, 1998]. Recently, several characteristic signatures indicating CMEs taking off near solar disk center have been discovered in short-wavelength emissions, imaged with Yohkoh and SOHO instruments. These images show that plasma structures described as "sigmoids" may precede eruptions of CMEs and that after a CME has left the corona, a pair of persisting patches of dimmed emissions may form on the opposite sides of a polarity inversion line [*Sterling and Hudson*, 1997; *Thompson et al.*, 1998; *Canfield et al.*, 1999; *Sterling et al.*, 2000]. The model of Gibson and Low is also able to relate these observed plasma structures qualitatively to the same CME internal magnetic field that reproduces the white-light morphologies of limb CMEs.

2.4. The CME Magnetic Flux Rope

The important point of the Gibson-Low model is that the three-part structure is due to a CME magnetic field

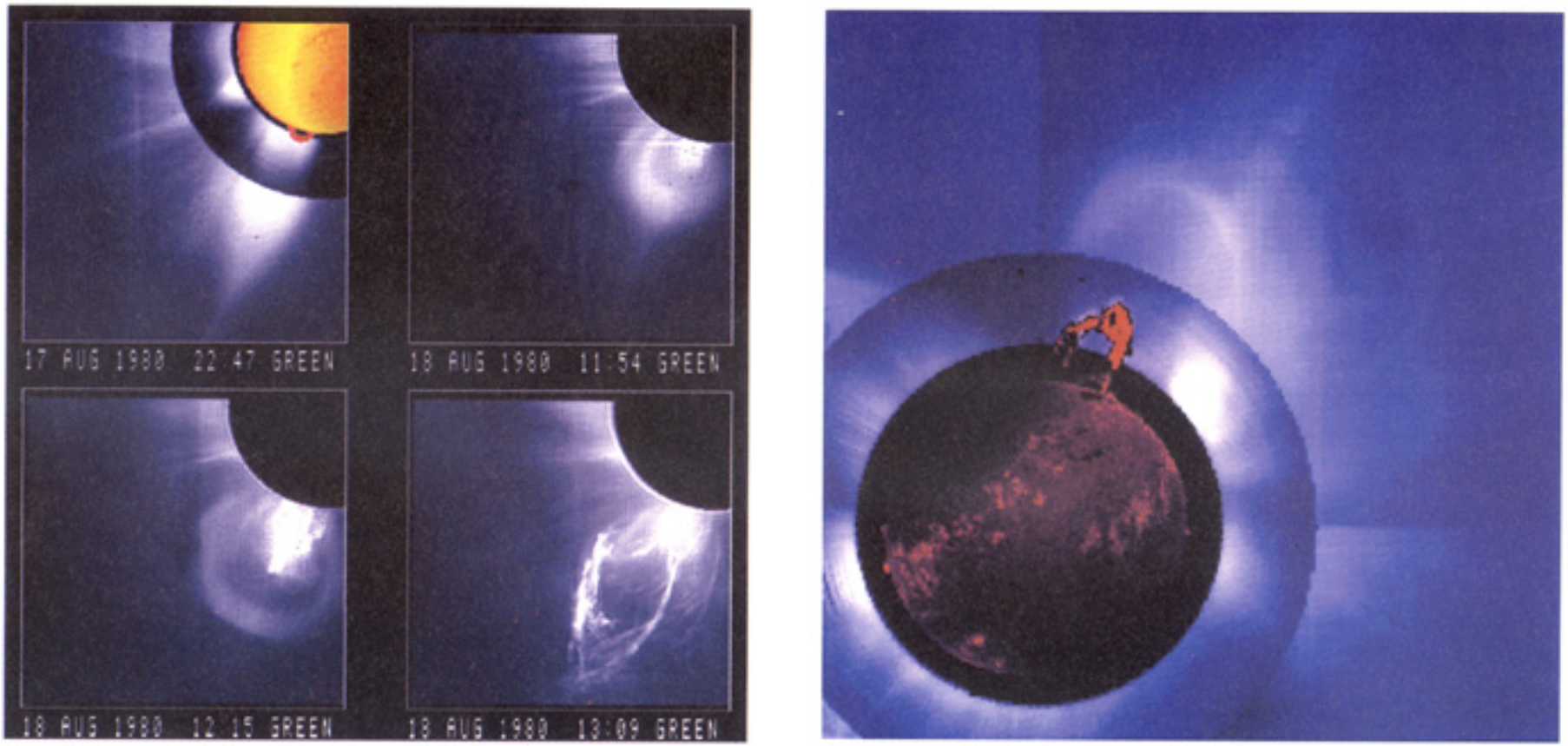

Plate 1. The August 18, 1980, and October 15, 1989, coronal mass ejections. The left four panels show the August 15, 1980, event in scattered white light observed with the NASA/SMM Coronagraph/Polarimeter (SMM C/P). The SMM C/P field of view is from about 1.5 to 6 $R_\odot$. The top left panel shows the corona before the CME eruption, extending the SMM C/P field of view inward to about 1.1 $R_\odot$ with a nearly simultaneous observation made with the Mauna Loa Solar Observatory (MLSO) Mark III Coronameter. Superposed is a full disk H_α, also taken at MLSO, showing a large quiescent prominence at the base of the helmet. The cavity of the helmet is not discernible because of image superposition. The three-part structure of the erupted CME is clearly seen in the panels for times 11.54 and 12.15. In the panel for 13.09, the bright CME leading front has traveled out of the field of view dominated at this time by the greatly expanded erupted prominence. The right panel shows the October 5, 1989 CME in a superposition of coronagraph white-light and H_α images, first published by *Hundhausen* [1997]. Shown against a blue background is the CME observed simultaneously with the SMM C/P and the MLSO Mark III Coronameter, combined with two H_α images in red. Of the H_α images, one is a full-disk image made at an earlier time before the CME eruption, showing an arch-shaped quiescent prominence located at the solar limb. Prior to eruption, this prominence sat at the base of the helmet streamer that upon eruption became the CME seen in white light. Superposed on this earlier image is another H_α image showing only the prominence, observed nearly simultaneously with the CME shown. At this time, the prominence had erupted and expanded in size to travel out behind the CME.

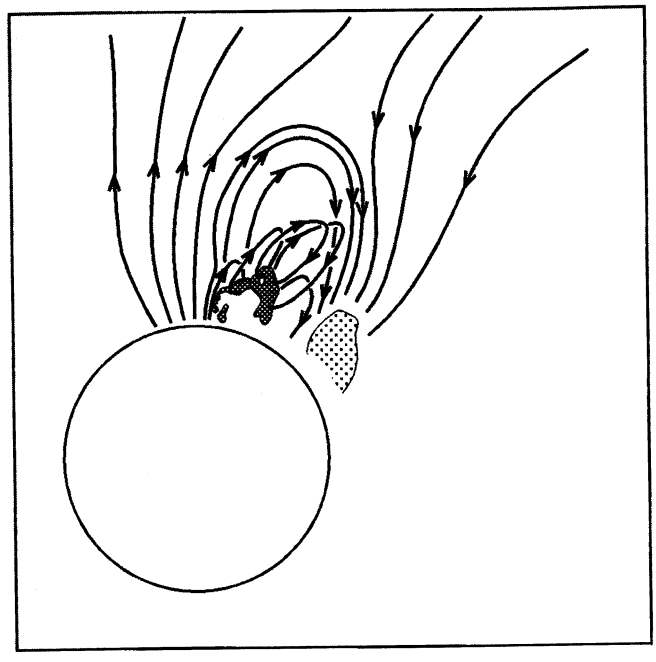

Figure 2. A sketch of the erupted prominence and the dense CME leading front of the October 15, 1989, event displayed in Plate 1. Superposed are arrowed lines, representing the lines of force of a theoretically proposed magnetic field associated with this CME. The external open magnetic field is shown to have been pushed aside by the outgoing CME dense front. Trailing this front are bipolar lines of force characterized with two ends attached to the coronal base. Behind the bright front is the cavity with a helical magnetic field threading into the erupted prominence. The tension force of the helical field "drags" the prominence out with the CME.

containing a flux rope of helical fields in the CME cavity. Figure 2 is a sketch of the global magnetic field expected in an observed three-part CME. Surrounding the cavity flux rope is the high-density leading front, containing a closed bipolar magnetic field anchored to the coronal base. Outside of the leading front the magnetic field is open, with one end out in interplanetary space and the other rooted to the coronal base. The CME is driven by the magnetic flux rope pushing its way out of the corona, lifting the mass in the leading front and stretching the embedded, closed bipolar fields of the front. The leading front is actually a shell of matter draped over a ball-like cavity containing the twisted flux rope [*Hundhausen*, 1987, 1999; *Webb*, 1988]. The loop-like appearance of the front end of the shell arises from limb brightening at the front in the optically thin corona.

Webb et al. [1997] had interpreted the October 15, 1989 CME in Plate 1 to be associated with a lengthy photospheric polarity-inversion line with a hairpin bend, which these authors have taken to imply a global quadrupolar magnetic field. Our alternative interpretation is that the CME magnetic field is locally bipolar. As interpreted in Figure 2, the CME is an erupted portion of a long narrow helmet-streamer belt over an equally long, curved polarity-inversion line. Crucial for the purpose of this review is the interpretation that the prominence prior to and during the eruption is suspended within a flux rope of twisted magnetic fields, a point that will gain significance as our discussion proceeds.

2.5. CME-Associated Flares

Observations show that three-part CMEs are associated with a particular kind of flare, the two ribbon flare in H_α in the chromosphere or the long-duration events of soft X-ray brightening in the corona [*Hundhausen*, 1999; *Kahler*, 1992]. When quality data are available to determine the temporal order of events, the CME has been reported to precede the associated flare, sometimes by a lapse of a fraction of an hour, or to occur almost simultaneously with the start of the flare [*Harrison*, 1986; *Hundhausen*, 1987, 1999; *Zarro et al.*, 1999].

Simultaneous observations with different instruments are crucial for establishing this kind of result. Yohkoh Soft X-ray Telescope (SXT) observations have revealed examples of plasma structures in motion prior to or simultaneous with heating interpreted to be due to magnetic reconnection [e.g., *Tsuneta*, 1997; *Ohyama and Shibata*, 1998; *Shibata*, 1999]. To relate these events to CMEs that generally occur on a considerably larger coronal scale, simultaneous white light observations to identify the associated CME events, if any, are essential. A recent comparison of Yohkoh SXT observations of flares with the associated CMEs observed by the SOHO/LASCO coronagraphs re-affirm the idea that CMEs have commenced or are already in motion by the time the associated soft X-ray flares begin [*Nitta and Akiyama*, 1999].

This temporal ordering of events can be explained by the two-step process sketched in Figure 3. A coronal helmet erupts into a CME to open up a belt of closed magnetic fields sandwiched between open polar fields in an idealized axisymmetric corona. The outgoing CME stretches the initially closed magnetic field of the helmet, under the condition of high electrical conductivity, into an open state. With the dominance of magnetic forces near the coronal base, the opened field collapses into a field reversal layer to form a thin electric current sheet. This is an ideal hydromagnetic process. The sheet forms because plasma is frozen into the magnetic field and there is not sufficient plasma pressure in the reversal layer to hold against the collapse of the layer. This proceeds to such a thin sheet that resistive reconnection sets in [*Parker*, 1994; *Kulsrud*, 1998], resulting in plasma heating and the reclosing of a part of the opened magnetic field [*Illing and Hundhausen*, 1983; *Hiei et al.*, 1993; *Webb and Cliver*, 1995; *Wu et al.*, 1997]. As is well known, this process fits observations of two ribbon flares and long-duration events well [*Hirayama*, 1974; *Kopp and Pneuman*, 1976; *Kahler*, 1992; *Hundhausen*, 1987, 1999].

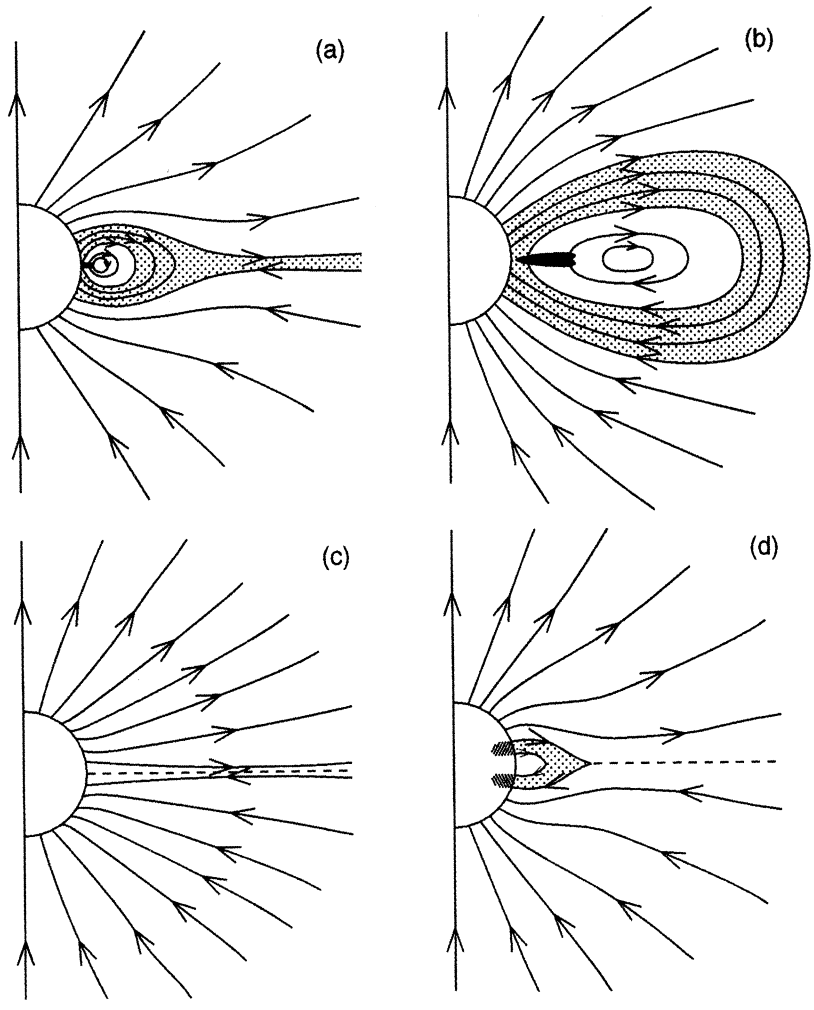

Figure 3. Two-step CME-flare process. The four sketches show magnetic lines of force in a poloidal plane of an idealized corona, taken symmetric about the polar axis, in a sequence of events represented as follows: (a) A coronal helmet streamer showing a high-density dome, threaded by a bipolar magnetic field anchored to the atmospheric base, with a cavity of detached magnetic fields, within which is a quiescent prominence represented by the bold line. The external magnetic fields are open into interplanetary space. For the purpose of this illustration the magnetic field is everywhere taken to be poloidal except in the cavity, where the twisted magnetic flux rope has a field component pointing out of the poloidal plane. (b) The ideal hydromagnetic expansion of the coronal helmet to produce the three-part CME. (c) The bipolar, poloidal, fully open magnetic field left behind by the CME, containing a field reversal layer indicated by the equatorial dashed line. (d) The global magnetic field partially reclosed via magnetic reconnection with flare-heated plasma in the newly closed (shaded) part of the field. The coronal helmet that reformed at the stage indicated in Figure 3d lacks the internal structure of a flux-rope cavity and quiescent prominence that characterize the coronal helmet in the initial state Figure 3a.

A basic feature in Figure 3 is that the first step releases ordered energy, bulk kinetic energy and work against gravity, whereas the second step liberates dissipated energy in the form of heat [*Low*, 1994]. The flare may initiate early, say, as soon as the current sheet forms [*Zarro et al.*, 1999], or may be delayed until circumstances favoring magnetic reconnection finally set in [*Harrison*, 1986; *Hundhausen*, 1987, 1999]. Moreover, the mass, speed, and specific (white-light) three-part morphology of a CME are not sensitive to the intensity of its associated flare [*Low*, 1981, 1984; *Feynman and Hundhausen*, 1994; *Hundhausen*, 1987, 1999; *Dere et al.*, 1999]. The CME and its associated flare are, in this sense, independent hydromagnetic processes [*Hundhausen*, 1999; *Low*, 1981, 1994]; see the debate between *Gosling* [1993a] and *Hudson et al.* [1993]. The following question thus arises: What causes a helmet streamer to erupt into a CME?

3. Helmet Streamers

The high thermal and electrical conductivities of the corona produce two competing dynamical effects that account for the large-scale features of helmet streamers and coronal holes such as seen in Figure 1.

3.1. Magnetically Open and Closed Coronal Regions

High thermal conductivity at the million degree temperature produces the solar wind [*Parker*, 1963; *Hundhausen*, 1972]. Electric currents sustained by high electrical conductivity produce the Lorentz force, comprising an isotropic pressure force and a tension force. The magnetic pressure enhances coronal expansion into the solar wind. The tension force is the only means to trap coronal plasma against expansion, provided the field geometry is right and the field intensity is sufficiently strong. This occurs in localized regions over a photospheric polarity inversion line. Here is where helmet streamers form, held in quasi-static equilibrium by the bipolar lines of force with foot points anchored on the two sides of the inversion line [e.g., *Li et al.*, 1998]. Outside the helmet are the coronal holes with their lines of force combed out into interplanetary space by the solar wind. The competition between solar-wind expansion and plasma trapping by closed bipolar magnetic fields creates a dichotomy of two states in the quiescent corona; the magnetically open coronal holes and the magnetically closed helmet streamers (see Figure 1 and Figure 4.

The typical magnetic field strength in the corona is about 10 G. This number is consistent with the divergence-free condition relating the observed microgauss interplanetary magnetic fields to their source in the corona [*Hundhausen*, 1972; *Parker*, 1963]. It is also the average field strength as indicated by the measured photospheric magnetic flux [*Parker*, 1979; *Priest*, 1982]. Although intense fields of 10^3 G are a common occurrence in active regions, these fields decay with height to much weaker fields, over length scales of the order of the sunspot size, so that in the low corona, fields of 100 G above the active region do not occupy great volumes in the corona. If a 100-G field is taken everywhere in the low corona, not only would the above observational constraints be violated, but also the global corona would be magnetically closed almost everywhere without the conspicuous coronal holes. A reasonable coronal field of 10 G still dominates over plasma pressure, but only near the base of the corona. At about 1-2 $R_\odot$ above, magnetic and plasma body forces are comparable, beyond which all magnetic lines of force are kept open by the solar wind.

The phenomenon of CME suggests that coronal helmets have different energy states, ranging from those that are ready to erupt into a CME, at one extreme, to the very stable states, at the other extreme. It is not just the eruptive energy that we need to be concerned with. The three-part structures of helmets ready to erupt indicate that their high energies are related to a certain common magnetic topology. The helmets that are far from being ready to erupt, such as one that has reformed after a CME (see Figure 4 and *Hiei et al.* [1993]), have only a simple bipolar magnetic field without the complex field topology of a cavity. It is this magnetic topology that makes the difference between helmet streamers in the two extreme energy states.

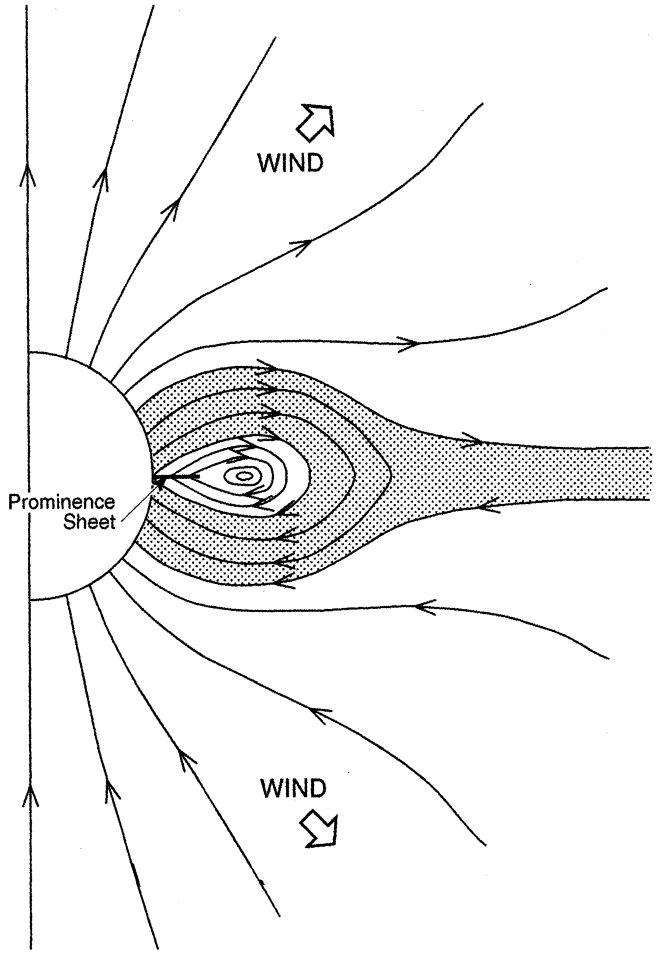

Figure 4. The idealized axisymmetric corona. Shown is a blown-up version of Figure 3a showing a magnetic flux rope running above the solar equator to encircle the Sun. The flux rope corresponds to those arrowed magnetic lines of force closed within the corona, with a significant azimuthal field component (pointing out of the poloidal plane). The quiescent prominence is shown as a locally radial sheet of cold matter trapped at the gravitational bottoms of the helical lines of force, where its weight is supported by the magnetic tension force. An azimuthal field component may also be present in the anchored part of the field outside the flux rope. The open field is strictly poloidal, since any azimuthal field component would have propagated out with the solar wind flowing in this magnetic region. The flux rope is held in equilibrium by the weights of the overlying helmet plasma and the prominence in the lower part of the flux rope. The solar equator is the polarity inversion line in this symmetrical atmosphere. The magnetic flux threading across the coronal base on the two sides of the equator arch over the equator high above the base to make room for the flux rope, a significant point in the text.

3.2. The Helmet Magnetic Flux Rope

There are outstanding observations of twisted magnetic structures in prominence eruptions and CMEs

[e.g., *Tandberg-Hanssen*, 1974, 1995; *Chen et al.*, 1997; *Dere et al.*, 1999; *Wood et al.*, 1999; *Ciaravella et al.*, 2000]. Suggestion of a preexisting flux rope in the solar atmosphere has been made by many workers to explain the prominence [*Chen*, 1989; *Priest et al.*, 1989; *Forbes and Isenberg*, 1991; *Vsrnak et al.*, 1991; *Choe and Lee*, 1992; *Isenberg et al.*, 1993; *Low*, 1993b; *Rust*, 1994; *Rust and Kumar*, 1994, 1996; *Low and Hundhausen*, 1995; *Schonfelder and Hood*, 1995; *Chen et al.*, 1997; *Wu et al.*, 1997; *Lionello et al.*, 1998; *Amari et al.*, 1999; *Gibson and Low*, 1998, 2000]. *Low* [1994] and *Low and Hundhausen* [1995] identified the magnetic flux rope not with the quiescent prominence, but with the cavity as observed in the corona, or with the H_α filament channel as observed in the chromosphere. This identification is crucial because the prominence is a linear structure, whereas the flux rope and its interpreted manifestation as the prominence cavity are both voluminous. The flux rope may or may not contain a quiescent prominence. Although the magnetic topology of a flux rope is perfect for trapping plasma condensations, whether a prominence forms in it presumably depends on the thermodynamic environment and mass content of the flux rope interior, as pointed out by Low and Hundhausen. This is consistent with the observation that the cavity or filament channel does not always contain a quiescent prominence [*Martin et al.*, 1994].

The above views are different from those others which postulate no pre-existing magnetic flux rope [e.g., *Antiochos et al.*, 1991]. In the latter, where a flux rope is observed in the eruption, it is considered to have been created by magnetic reconnection taking place during the eruption.

By a flux rope is meant a field with lines of force winding about each other a full turn or more in the corona between photospheric foot points [*Low*, 1996]. In contrast, the bipolar field threading the dense helmet dome has lines of force that do not wrap around each other more than a turn. The simplest kind of magnetic flux rope is the one in Figure 4. In this idealized axisymmetric corona, the rope runs around the entire Sun, completely detached from the base of the corona; see the numerical model of *Guo and Wu* [1998]. This sketch has only pedagogical value in making a topological distinction between rope and anchored bipolar fluxes.

A flux rope completely closed in the corona may exist over a localized region above the photosphere. One example is that of a circular torus of winding helical fields levitating horizontally with its internal axis forming a circle parallel to the coronal base. It is held down all

Figure 5. The handedness of quiescent prominences. These sketches of H_α filaments and their surrounding chromospheric fibrils seen on the disk have been adapted from *Martin et al.* [1994]. The characteristic streaming of the fibril lines on the two sides of a filament in Figure 5a and 5b correspond to the dextral and sinistral configurations, respectively, defined by Martin et al. An observer standing on the positive magnetic-polarity side of a filament and facing the filament sees a dextral, or sinistral configuration if the fibrils on that side stream to the right or left, respectively. In Figure 5c, the arrowed magnetic lines of force around the sinistral filament Figure 5b are added, seen in projection on the solar disk, in accordance with the interpretation of a flux-rope model for the filament given by *Low and Hundhausen* [1995]. In this interpretation the filament is a condensation supported by the tension force of helical lines of force forming the flux rope. Such helical lines are located under arches of bipolar lines of force with two ends anchored at the coronal base on the two sides of the filament. See the text to relate this magnetic topology to the two-dimensional idealization shown in Figure 4. This sinistral filament naturally has a right-hand twist in the encasing magnetic flux rope. The dextral filament in Figure 5a corresponds to a left-hand twisted flux rope not shown.

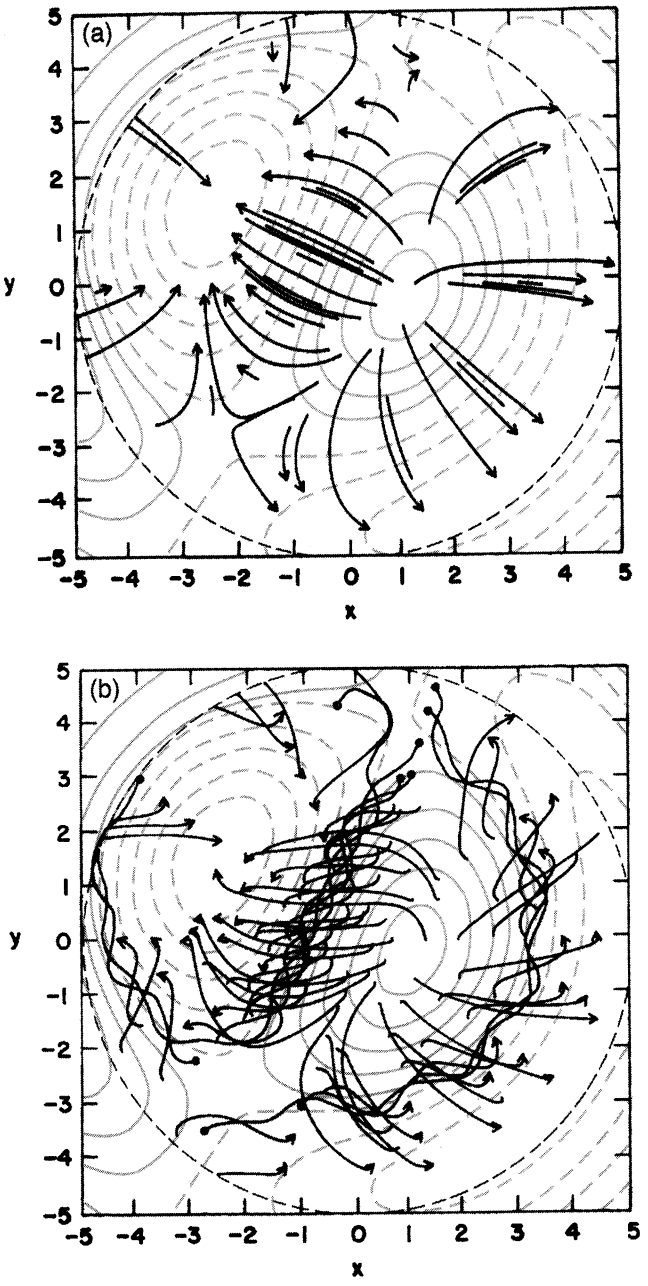

Figure 6. Exact magnetostatic equilibrium solution. The two panels show plots of arrowed lines of force seen in projection on the solar disk associated with the same distribution of normal magnetic flux at the coronal base displayed as (unarrowed) contours of constant normal flux. The contours are solid and dashed to indicate positive and negative polarities, respectively. The upper panel shows a potential magnetic field in a plane-parallel hydrostatic atmosphere. The lower panel shows a nonpotential magnetic field in equilibrium with a structured atmosphere where a density enhancement, not shown, is supported by magnetic lines of force which are anchored at two ends to the atmospheric base but such that a subset of these lines form a flux rope over the polarity inversion line, lines that wrap over each other more than one turn within the atmosphere. The two magnetic fields are exact hydromagnetic solutions taken from *Low* [1992].

along the length of the torus by arches of bipolar field lines anchored to the photosphere. Such a flux rope may be the origin of some quiescent prominences that form a closed circular curve (see *Martin et al.* [1994]). More common flux ropes have lines of force anchored to the photosphere as they wrap several turns around each other in the corona. Figure 5 shows a sketch of such a flux rope magnetic field in realistic geometry associated with a quiescent prominence of the type discussed by *Martin et al.* [1994]. Figure 6 shows exact mathematical solutions taken from *Low* [1992] as an assurance that the sketch in Figure 5 is theoretically admissible. Other exact solutions illustrating similar flux rope field topologies can be found in the prominence models of *Lites et al.* [1995], *Lites and Low* [1997], *Gibson and Low* [2000] and *Aulanier and Demoulin* [1998].

The flux rope magnetic field explains many observed features of the helmet. As in the CME, the enhanced magnetic pressure of the flux rope makes up for the depleted plasma pressure in the helmet cavity. The suppression of thermal conduction across the magnetic field, combined with the long thermal paths of winding field lines, suggest that the interior of the flux rope is thermally isolated. This environment may promote a variety of condensation instabilities to create self-consistently the evacuated low density of the cavity and the quiescent prominence within it [*Smith and Priest*, 1977; *Mason and Bessey*, 1983; *Low and Hundhausen*, 1995]. This analysis shows that the boundary between the dense helmet dome and the cavity must be sharp, as observed; see Figure 7. This boundary is the magnetic flux surface separating the flux rope from the topologically different, bipolar field of the helmet dome.

3.3. Energy Storage in a Magnetic Flux-rope

The magnetic flux rope also explains the energy needed to expel a CME and to produce a post-CME flare [*Low and Smith*, 1993; *Wolfson and Dlamini*, 1997, 1999; *Wolfson and Saran*, 1998]. The question of the availability of free magnetic energy to drive a CME is nontrivial. A 10-G potential magnetic field in a volume of the size of a typical helmet contains a total energy comparable to the CME/flare energy of about 10^{32} *ergs*, but none of it is available for release.

Force-free magnetic fields anchored at photospheric footpoints generally do not have enough energy to spontaneously open up [*Aly*, 1984, 1991; *Sturrock*, 1991]. In physical terms, the limit is related to the conservation of flux which implies that when an anchored, bipolar field should open up into the atmosphere, it would fill up a greater volume without significantly diminishing its field intensity in the main part of that volume. This means that the total field energy needs to increase with the opening process, showing that such a field has no energy to provide a CME.

Intriguing processes to circumvent the constraint of Aly on the spontaneous opening up of force-free mag-

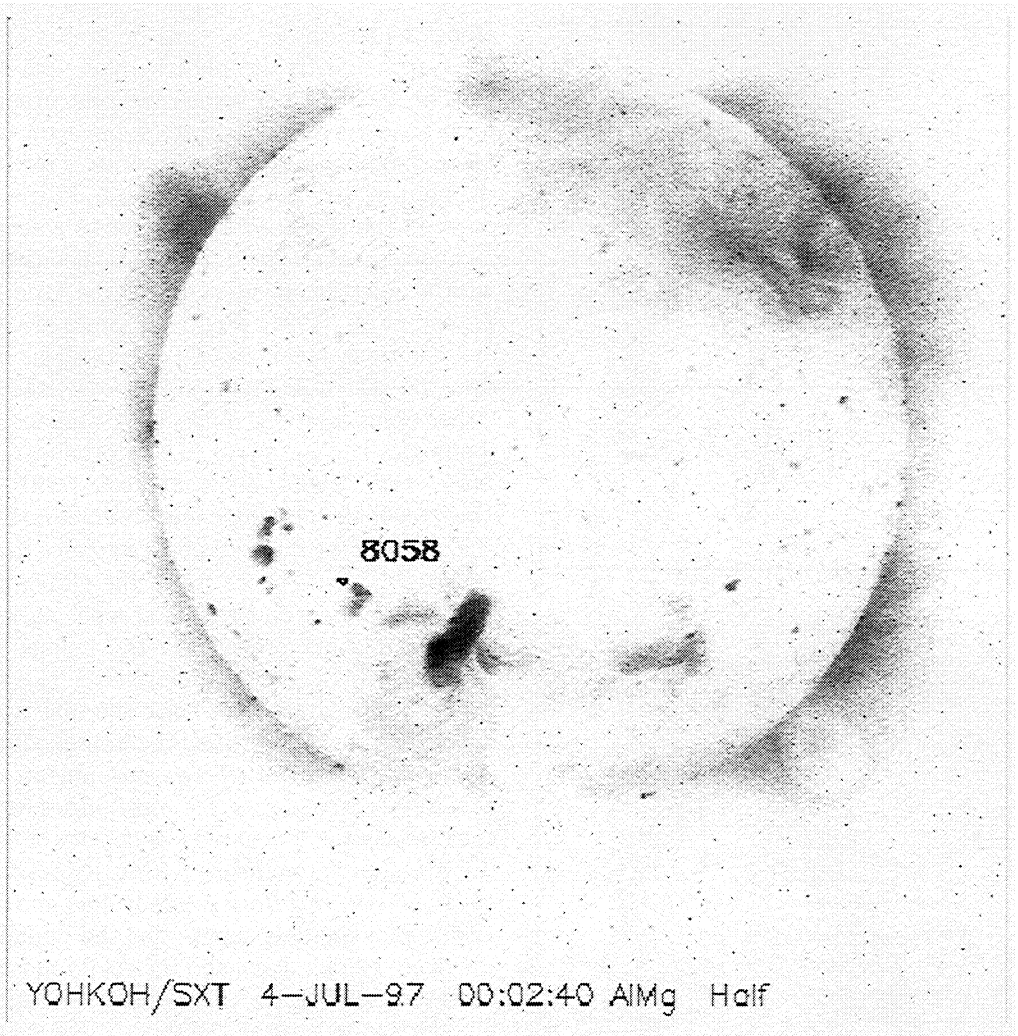

Figure 7. A helmet cavity in soft X-ray. This full-disk corona imaged with the Yohkoh soft X-ray instrument on July 4, 1997, shows, at the southwest limb, a roundish cavity of reduced emissions. The bottom of its especially sharp boundary appears to touch the solar limb tangentially. *Harvey and Gaizauskas* [1998] and *Hudson et al.* [1999] have complementary data to show that this cavity corresponds to a filament channel within which a massive quiescent prominence is found.

netic fields have been proposed [*Wolfson*, 1993; *Lin et al.*, 1998; *Antiochos et al.*, 1999]. While these processes are interesting in their own rights, it is important to note that exceeding the energy of the open configuration is, in principle, possible, even for a force-free field [*Low and Smith*, 1993]. This possibility obtains if a part of the magnetic field is completely detached from the photosphere, such as in the case of a horizontally levitating flux rope mentioned above. The entire rope can leave the atmosphere to expand and give up its magnetic energy. Only the anchored part of the magnetic field stays behind. A sizeable flux rope in the initial state must occupy a space out of which the anchored part of the magnetic field is displaced; see Figure 4. The expulsion of the flux rope vacates this space, into which the compressed anchored field can expand. Elementary magnetostatic solutions have shown how this feature enables magnetic flux ropes to store enough magnetic energy for opening up magnetic fields in a CME process.

3.4. Confinement of Magnetic Flux Rope

The case is tidy and clear with fully detached flux ropes but remains valid with the more common flux ropes comprising lines of force which are attached to the coronal base; see Figure 5 and Figure 6. This can be seen in general terms by an application of the hydromagnetic virial theorem [*Chandrasekhar*, 1961; *Low and Smith*, 1993; *Low*, 1999b] to show that twisted magnetic fields in an unbounded atmosphere need to be confined by an external relatively untwisted field, or by the weight of the atmosphere, or both.

Figure 8 makes that basic physical point without dealing with the mathematics of the virial theorem. Consider a magnetic field in axisymmetric geometry outside a unit sphere. Figure 8 shows three possible field topologies: a field with all lines anchored to the inner boundary; a field with no lines anchored to the boundary; and a field with a flux closed in the space

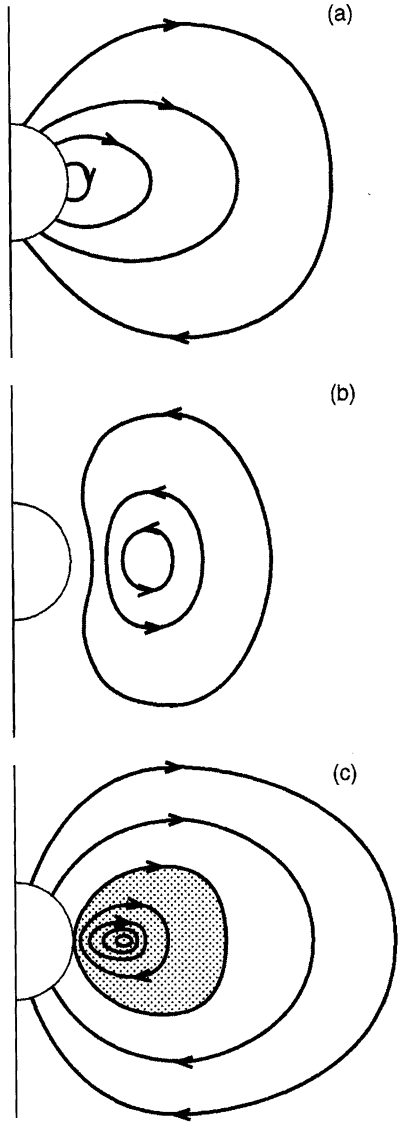

Figure 8. Three topologically possible states for the axisymmetric magnetic fields in the unbounded atmosphere. Shown are the projections of the magnetic lines of force onto the poloidal plane. In each case the field has an azimuthal component pointing out of the poloidal plane. The three cases are (a) a field with all lines of force anchored to the inner spherical boundary, topologically accessible by the foot point displacement of a potential magnetic field; (b) a field with no lines threading across the inner spherical boundary, with no possibility of force-free equilibrium as described in the text; and (c) a field containing both an anchored bipolar flux and a fully detached flux. The ratio of the fully detached flux to the anchored flux may not be too large for a force-free equilibrium to exist.

outside the sphere but surrounded by another flux anchored to the inner boundary. In the third possibility, let R_{flux} be the ratio of the closed flux to the anchored flux. Now suppose the three fields are twisted, with a significant azimuthal field component, and the medium is so tenuous that the fields are force-free with the electric current density parallel everywhere to the field **B**:

$$(\nabla \times \mathbf{B}) \times \mathbf{B} = 0. \tag{5}$$

The virial theorem then states (1) that equilibrium with topology (a) may exist; (2) that equilibrium with topology (b) cannot exist; and (3) that equilibrium with topology (c) may exist provided the ratio R_{flux} is less than some critical value to be determined by calculation. In the force-free approximation a magnetic flux rope everywhere not connected to the atmospheric base has no equilibrium and must expand in all directions, except when it is confined by a surrounding anchored magnetic field of some required strength.

In this context the observation of Poland and MacQueen (1981) is intriguing. They described a CME erupting out of a helmet streamer following a weakening of the photospheric magnetic field at the base of the helmet. This observation would be consistent with a failure to confine the cavity flux rope by the reduction of the helmet magnetic flux anchored to the photosphere.

In the solar corona, over the length scales of helmet streamers, gravity and pressure are important. The weight of the atmosphere in this case provides an additional means to confine a detached magnetic flux rope. A much larger ratio R_{flux} is possible compared with the case of a force-free magnetic field. In a helmet streamer containing a cavity, the circumstance is that of a suppression by several confinement agents of the expulsion tendency inherent in the cavity magnetic flux rope. There are four confinement agents evident in Figure 4: the weight of the helmet dome over the cavity; the weight of the prominence suspended in the cavity; the magnetic tension force associated with the anchored bipolar field of the helmet dome; and the greater magnetic pressure of the open magnetic field outside the helmet streamer. A CME results from the failure of the cavity flux-rope to be confined. The key to understanding CME initiation thus lies in a hydromagnetic theory of the helmet streamer that can explain how this confinement could be stable in some circumstances and unstable in others [*Low and Hundhausen*, 1995].

From phenomenology, CMEs must involve instabilities of a special kind, namely, those that run away into a global expulsion once initiated. A hydromagnetic system generally exhibits a rich variety of instabilities, not all relevant to the CME. For example, a kink instability does not necessarily imply a CME since it may just produce local reconnection to bring about a stable energy state as the system remains gravitationally bound. Confined flares are examples of this kind of instability. The instability producing a CME must, in our synthesis, be one that enables the cavity flux rope to break loose. Once it has broken loose, the loss of confinement of the flux rope epitomized in Figure 8b, naturally leads to the global outward expansion of a white-light CME.

Of the confinement agents, the weight of the quiescent prominence has some interesting effects which merit further discussion. Drainage of plasma from a prominence in its stable phase is commonly observed [*Tandberg-Hanssen*, 1974]. Drainage may be due to local bal-

looning interchange instabilities [*Fong*, 1999]. *Athay* [2001] recently reminded us that the global corona may be subject to changes in heating and local cooling on very small scales to result in plasma "raining" down and presumably crossing magnetic fields by resistive interchange instabilities. This plasma rain may make up for prominence mass-loss via drainage. The quiescent prominence is thus not a true static object but is maintained in some delicate balance of energy and mass [*Tandberg-Hanssen*, 1995]. When that balance is not maintained, the prominence may gain or lose weight, the latter with dramatic consequences if the prominence is a crucial part of the confinement of a magnetic flux rope. As the lightening of the prominence gradually corrupts the rope confinement, the rope eventually would break loose and erupt. Alternatively, without the prominence losing significant weight, magnetic twist may monotonically accumulate in the cavity flux rope through emergence of fresh magnetic flux at the coronal base. When the existing confining forces become inadequate, the flux rope would break loose.

Once a prominence erupts the drainage is often enhanced, as is commonly observed in H_α [*Rusin and Rybansky*, 1982; *Lipscy*, 1998; *Vsrnak*, 1998; *Gopalswamy and Hanaoka*, 1998; *Gilbert et al.*, 2000]. This lightening of the prominence during the initial phase of a CME event may account for the gradual acceleration starting from a low initial speed, which characterizes prominence-associated CMEs [*MacQueen and Fisher*, 1983; *St. Cyr et al.*, 1999]. The drainage may also explain the relatively small masses of the erupted prominences inside most CME cavities. Generally, the erupted prominence is an order of magnitude less massive than the leading bright front of the CME, the latter mass to be identified with the coronal mass in the dome of the erupting helmet.

Exceptions to this general result are rare, but significantly, they exist. The August 18, 1980 CME event in Plate 1 [*Illing and Hundhausen*, 1986; *Rusin and Rybansky*, 1982] and the SOHO/LASCO event reported by *Gopalswamy and Hanaoka* [1998] are two outstanding exceptions. In both events the prominence had an estimated mass in excess of 5×10^{16} g prior to eruption. Despite copious drainage during the eruption, as much as 10^{16} g went out in the ejected part of the prominence to be detected by the respective spaceborne coronagraphs. The significance of these two events is that the prominence as a confinement agent may be as important as the helmet dome. Mass estimates using H_α are approximate because of the unknown prominence filling factor. More reliable methods of estimating the masses of prominences [e.g., *Gilbert et al.*, manuscript in preparation, 2000] will be helpful to quantify more tightly how much mass resides in a quiescent prominence and how much is drained during eruption.

The drainage of plasma to release a flux rope may take place even more energetically deep within an active region. The intense magnetic fields in an active region require very dense plasma at the photosphere to hold the fields in place. The impulsive "dropping of anchor" via drainage of dense plasma associated with the release of such intense magnetic fields into the corona may generate helioseismic waves at the photosphere. One event of impulsive generation of helioseismic wave has been observed and interpreted to be caused by the heating of an impulsive flare [*Donea et al.*, 1999]. It will be interesting to search observationally for similar impulsive helioseismic events that may result from the drainage of heavy plasma low in the atmosphere in association with a sudden release of a flux rope.

4. Flares and Long-lived Structures

What is the origin of coronal magnetic flux rope? It has been proposed that magnetic flux ropes may form out of a preexisting, coronal magnetic field [e.g., *van Ballegooijen and Martens*, 1989; *Choe and Lee*, 1992]. While these ideas are interesting, coronal phenomenology described in this review suggests a subphotospheric origin.

4.1. Flares and Heating

Astrophysical large-scale magnetic flux, once created, cannot be destroyed readily. Only its field topology can be changed through current-sheet formation and reconnection [*Parker*, 1979, 1994; *Priest*, 1982]. Most solar imaging instruments have a limit of spatial resolution of the order of 10^3 km. The time to resistively dissipate a magnetic field of that observable smallest scale in the million-degree corona exceeds 10^3 years, long compared with Afvenic transit times typically of the order of seconds to hours. Resistive dissipation via magnetic reconnection occurs readily in the corona over extremely small scales at the fast timescales despite the high conductivity [*Parker*, 1994; *Kulsrud*, 1998]. These processes rapidly drain away the free energy of the large-scale magnetic field but cannot destroy the large-scale field. The free energy runs out in a matter of hours, and the persistent large-scale field must reach some kind of stable macroscopic equilibrium. The macroscopic equilibrium is only approximate in the sense that small-scale reconnection continues with liberation of small amounts of energy even as the already energy-depleted, large-scale field becomes quiescent [*Parker*, 1994].

These general theoretical considerations put solar flares into at least three classes. The first class contains flares arising from the emergence of new magnetic flux which reconnects with the preexisting magnetic flux in the corona. Each flare sheds excess magnetic energy with changes of magnetic topology, to enable the two flux systems to combine and reach a metastable state.

The second class of flare coalesce magnetic flux systems, already emerged in the corona, as they come together by slow evolution characterized by the typically

0.5 $km\ s^{-1}$ photospheric plasma flow. These flares reconnect to simplify the topology of combined magnetic fields, typically the fields found in a solar active region. Separate sunspot groups may thus combine, with flares punctuating an otherwise slow evolution. When the sunspots eventually decay, a more diffused larger-scale magnetic field is left behind penetrating into the larger volumes of the corona [*Lites et al.*, 1995].

The third class of flares are the small-scale reconnection activities that persist in quiescent large-scale magnetic fields, the nanoflares and microflares which heat the corona locally [*Parker*, 1994; *Judge et al.*, 1998; *Longbottom et al.*, 1998]. Except for the length scales of the processes and differences in the amounts of magnetic energy released to heat the atmosphere, these three classes of flares involve the same basic physics.

4.2. Solar Magnetic Helicity

The interesting question to ask is, After a flare, is there any significant free energy left in the relaxed large-scale field? In other words, is there a hydromagnetic constraint that forbids a certain amount of free magnetic energy from being flared away? From studies of hydromagnetic turbulence, magnetic helicity is just such a constraint capable of trapping magnetic free energy [*Taylor*, 1986; *Heyvaerts and Priest*, 1984; *Ruzmaikin and Akhmetiev*, 1994; *Montgomery and Bates*, 1999]. We refer the reader to *Low* [1999b] and *Berger* [1999] and references therein for a pedagogical discussion of the application of magnetic helicity to the solar atmosphere. For our purpose here, two basic points are needed.

First, magnetic helicity is a measure of twist in magnetic fields [*Moffatt*, 1978]. It is absolutely conserved if the electrical conductivity is infinite. It is approximately conserved if the conductivity is very large in the sense of a large magnetic Reynolds number R_M, the dimensionless ratio between the characteristic speeds of plasma bulk motion and resistive diffusion of the large-scale field. In the corona, R_M is of the order of 10^{15-18}. In this physical regime, repeated magnetic reconnections in a fully developed turbulent plasma do not preserve magnetic helicity but transfer this quantity from one localized part of the medium to another such that summed over a large-scale volume, the total magnetic helicity remains approximately conserved during reconnection. Another way of stating this theoretical result is that during a flare, magnetic energy is liberated rapidly compared with the loss of magnetic helicity [*Berger*, 1984]. This means that once flaring is finished, over a few hours, the relaxed magnetic field must contain approximately the same total magnetic helicity. If the conserved total magnetic helicity is zero, the relaxed state may be a potential field with no free energy. Otherwise, the relaxed magnetic field must retain some free energy associated with the nonzero conserved total magnetic helicity, and if that helicity is large, a flux rope of twisted fields forms naturally as an end product. In the latter, flaring has been forbidden to release all the free energy.

The second point to make is that the theory for the above phenomenological conclusion is intricate and technically difficult. The magnetic helicity density is defined by

$$h = \mathbf{A} \cdot \mathbf{B} , \tag{6}$$

where $\mathbf{A}$ is the vector potential of the magnetic field $\mathbf{B}$. Since $\mathbf{A}$ has a free gauge, additional theoretical constructs are needed to ensure gauge invariance for proper use of this formula [*Moffatt*, 1978; *Berger and Field*, 1984]. We proceed with our discussion without dealing with the issues of gauge invariance.

If conservation of magnetic helicity is accepted, a set of observations about solar magnetic structures becomes significant. For over half a century, researchers have observed that magnetic structures in the solar atmosphere tend to be predominantely of the left-hand and right-hand twists in the Northern and Southern Hemispheres, respectively. This is seen in the swirl of H_α chromospheric structures around a sunspot; prominence structures; the electric current helicity of measured photospheric vector magnetic fields; and, the handedness of magnetic clouds in interplanetary space identified with CMEs coming from the two hemispheres [*Richardson*, 1941; *Leroy*, 1989; *Seehafer*, 1990; *van Ballegooijen and Martens*, 1990; *Martin et al.*, 1994; *Bieber and Rust*, 1995; *Bao and Zhang*, 1998; *Pevtsov and Canfield*, 1999; *Zhang and Bao*, 1999]. Most notable is the discovery of *Martin et al.* [1994] that H_α prominences have two basic configurations given the terms "dextral" and "sinistral". Figure 5 describes these two configurations as defined by Martin et al., and relates them to the twists of the magnetic flux ropes containing the prominence [*Low and Hundhausen*, 1995]. This hemispherical preference of handedness is independent of solar cycle [*Martin et al.*, 1994]. This result is not surprising theoretically because magnetic helicity depends quadratically on the field so that globally reversing the sign of a magnetic field at the end of an 11-year cycle does not necessarily require a change of sign of its helicity.

To make hydromagnetic sense of these magnetic observations, let us postulate that magnetic flux emerges into the corona in a state of significant twist, as suggested by observations and theory [*Kurokawa*, 1987; *Leka et al.*, 1996; *Emonet and Moreno-Insertis*, 1998; *Ishii et al.*, 1998; *Linton et al.*, 1998; *Fan et al.*, 1999; *Manchester*, 2000]. The twist in the emerged magnetic field is predominantly negative in the Northern Hemisphere and positive in the Southern Hemisphere, to fit with the observed hemispherical preference of the sign of the twist. This postulate implies that the mechanism producing the magnetic twists in the solar interior is a global process, so that over the scale of the size of the Sun, the magnetic helicities in the two hemispheres

would mutually cancel [*Bieber and Rust*, 1995]. Processes localized within a hemisphere, say, within a localized convective cell, would produce twists of both signs to conserve helicity in that localized volume. Such processes do occur, of course, but they cannot contribute to the global effect of hemispherical sign preference; see the discussion by *van Ballegooijen and Martens* [1990].

We do not yet have a dynamo theory to account for the twists postulated to be present in emerging fluxes, but the postulate has the following far-reaching implication when coupled with the conservation of magnetic helicity. As more and more magnetic structures emerge into the atmosphere during a solar cycle, their flares can only get rid of a part of their free energies while their largely like-signed magnetic helicities add cumulatively in the coalesced structures within each hemisphere. The free energy trapped by magnetic helicity also accumulates. The accumulation of magnetic helicity continues with the same sign in each hemisphere into the next solar cycle despite the reversal of the field. Thus we arrive at a physically untenable situation of an unbounded increase of both magnetic helicity and trapped energy in the two hemispheres, as the solar cycles progress.

4.3. Corona As an Open System

The resolution of this situation drives home the fact that the corona is an open system, in contrast to laboratory plasmas confined within rigid containers. Whereas in the laboratory magnetic fields are always destroyed resistively when no longer needed, by cutting off the power supply, no similar process is relevant to large-scale astronomical magnetic fields except by an expulsion of an entire body of magnetic field out of the open system [*Low*, 1999b]. If not for bodily expulsion, a large-scale field once created will persist for time exceedingly long compared with characteristic dynamical timescales. Large-scale structures as products of flares and flux emergence do persist in the corona, namely, the helmet streamer belts and their cavity flux ropes. However, these structures must meet certain conditions for the confinement of their magnetic fields, as discussed in section 3.4. Whenever confinement conditions fail, a helmet streamer breaks into a CME only to reform another helmet that meets these conditions.

If flux emergence can be stopped permanently, the hypothetical corona would have blown its last CMEs, with the remnant structures of the corona persisting with no activity for an exceedingly long time, so long as its million-degree temperature and high electrical conductivity are maintained. In the real corona, flux emergence in each magnetic cycle drives the solar corona relentlessly by monotonically increasing the magnetic helicity in the atmosphere. This is the reason for helmet streamers to have a relatively short lifetime, of the order of a full solar rotation at activity maximum, when each may be expected to violate confinement conditions and blow off as a CME.

Whereas relentless flux emergence leads to unbounded injection of magnetic helicity in each hemisphere, the one principal means of magnetic-field confinement, namely, plasma weight, has a clear limit. There clearly can be no more weight available for field confinement than the total weight of the low corona of the order of 10^{17} g [*Tandberg-Hanssen*, 1974; *Athay*, 2001]. The upper bound of observed CME masses, including the rare cases of very massive erupted prominences, is of the order of 2×10^{16} g, roughly about 10% of the total coronal mass. It will be interesting to derive this upper bound from a hydromagnetic calculation of the failure of field confinement under typical coronal conditions.

The breaking loose of the cavity flux rope to open up its surrounding magnetic fields during a CME sets the stage for a final magnetic reconnection in the lifetime of that rope. The post-CME flare produced by reconnection to reclose the opened field fits neatly to complete a pretty picture. The expulsion of the flux rope takes with it much of the magnetic twist trapped in the helmet; but see the opposing point of view given by *Gosling* [1999]. It leaves behind an open field along which twist can propagate out as Alfven waves. Reconnection then produces a largely untwisted, helicity-free helmet streamer [*Hiei et al.*, 1993; *Hundhausen*, 1999; *Sterling et al.*, 2000]. Our analysis therefore singles out such CME-related flares to belong to a fourth class of flares in their own right. Whereas the first three classes are confined flares, each conserving magnetic helicity, the flares of the fourth class lose their helicities, not by resistive dissipation but by ideal transport out of the corona into interplanetary space.

5. CMEs and the Solar Dynamo

We are now able to say definitely what the role of CMEs is in solar activity. That role is less to remove mass as it is to remove magnetic flux and magnetic helicity that have made their way into the corona. A CME culminates an involved process of magnetic flux transport that begins with emergence of new magnetic flux from the solar interior into the solar atmosphere. A significant part of the emerged flux bodily gets into the corona to first persist as a long-lived magnetic flux rope and then, finally, to be expelled into interplanetary space as a CME. The mass that is expelled in the CME is not arbitrary but is determined by the requirements of flux-rope confinement prior to eruption.

A similar process of flux and helicity ejection was made independently by *Rust* [1994], deriving from the phenomenology of eruptive prominences and observations of magnetic clouds in interplanetary space. In the physical picture first given by *Low* [1994], made more complete in this review, the flux rope is identified with the much larger scale cavity within the coronal helmet and is the central link among the different components of solar activity.

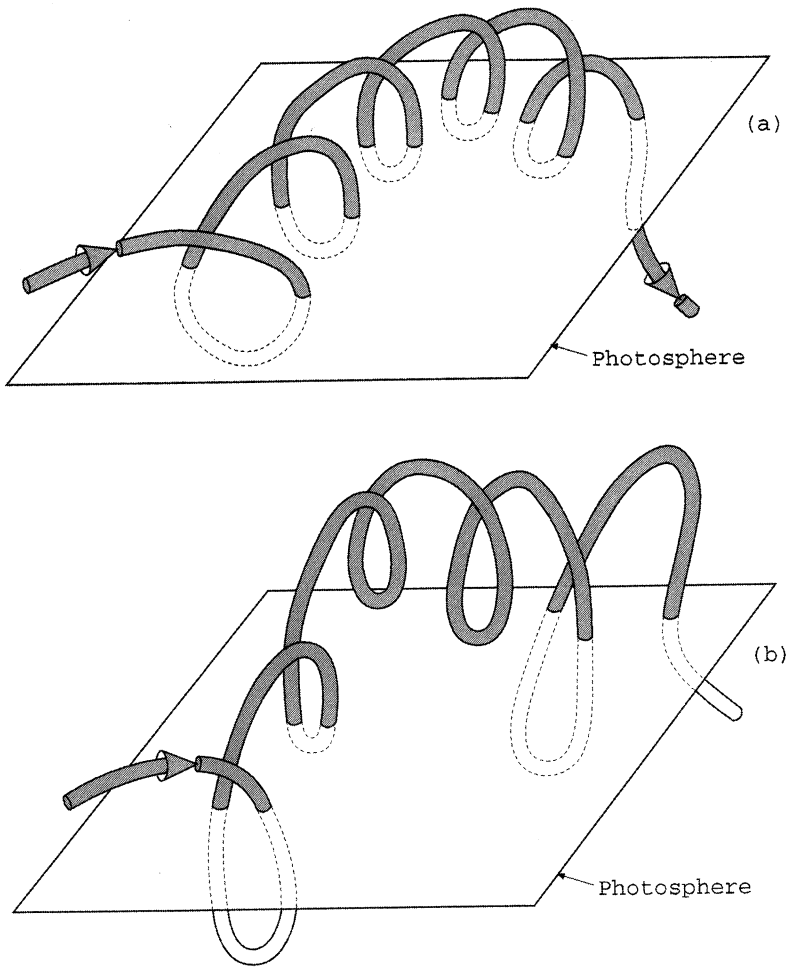

Figure 9. Emergence of a magnetic flux rope. A single helical flux tube of a twisted flux rope is shown in two stages of emergence across the photosphere represented as a plane. The other intertwining flux tubes of the flux rope are not shown in order to keep the sketches simple. The intertwining among the flux tubes should be kept in mind as a constraint against the relaxation of the single tube shown in this figure into a straight flux tube. In Figure 8a, bipolar arches rooted to the photosphere are shown to be the result of inverted-U portions of the helical field having risen through the photosphere. Siphon flows along the flux tube driven by pressure imbalance readily result in the lightened parts of the helical tube to buoyantly rise through the photosphere and other overly heavy parts to sink below the photosphere. In Figure 8b, two U-shaped parts of the flux tube are shown to have risen above the photosphere; a third U-shaped part is in the process of rising above the photosphere; and others loaded with drained material have sunk deeper below the photosphere. Each rise of a U-shaped part of the flux tube above the photosphere is accompanied by a clean annihilation, observed at the photosphere, of a pair of opposite magnetic-polarity patches. This annihilation reduces the magnetic flux of each sign across the photosphere.

5.1. Bodily Escape of Magnetic-Flux Systems

The question is crucial whether it is physically possible for a main part of a flux system to make its way bodily into the corona [*Golub et al.*, 1981; *Spruit et al.*, 1987; *Manchester*, 2000]. Future observations will be essential for a definitive answer. For the present, the theoretical reason is persuasive that such bodily flux transport must occur, as illustrated in Figure 9. The behavior depicted in Figure 9 is not some complex hydromagnetic property but is due to the interplay between helical field topology and magnetic buoyancy, basic effects governing a magnetic field in a stratified atmosphere.

For the intense and well organized field in Figure 9, its passage through the photosphere may be directly observed [*Lites et al.*, 1995]. More commonly, the emerging magnetic field is highly tangled, churned by the fluid-dominated layers below the photosphere [*Low*, 1996]. Its passage through the photosphere is then not so easily detected as a large-scale twisted structure. In this case the inherent twisted topology represented by its conserved total magnetic helicity remains hidden in

the tangled field until the flux system has arrived in the corona. Dominating over the tenuous coronal plasma, the different parts of the complex field would press into each other to flare. Flaring simplifies the field's tangled topology to produce a large-scale flux rope that finally reveals the conserved magnetic helicity. This flux rope becomes observable as coronal cavities and H_α filament channels [*Serio et al.*, 1978; *Low and Hundhausen*, 1995; *Harvey and Gaizauskas*, 1998; *Hudson et al.*, 1999].

Figure 9 shows two observable consequences. An inverted-U flux tube moving up through the photosphere from below creates a pair of bipolar magnetic foot points on the photosphere that move apart. A U-shaped flux tube with the bottom of the U lifting off from below the photosphere brings a pair of bipolar magnetic sources to mutually annihilate, completely and cleanly, as seen at that level. The first process produces new magnetic flux penetrating the photosphere. The latter process removes magnetic flux already penetrating the photosphere. Figure 9 shows that the rise of a magnetic flux rope through the photosphere must involve the latter process; that is, it is associated with flux removal from the photosphere.

In the more common process of a field churned into a complicated tangle, the rise of the magnetic system through the photosphere involves a complexity of small-scale U-loops lifting off through the photosphere. Topologically, the process is similar to the one depicted for the organized rope in Figure 9. The important consequence in either case is that the cavity flux rope that forms at the base of a coronal helmet involves removing a certain amount of flux previously threading across the photosphere at the base of the helmet [*Low*, 1997].

5.2. A Numerical Estimate

The following estimate first proposed by Arthur Hundhausen illustrates how much magnetic flux might be so removed from the photosphere. Suppose the the creation of a cavity flux rope at the base of a helmet removes an amount as modest as 1% of the flux of a chosen sign threading across the base of the helmet. Then 100 CMEs are needed to remove the flux across the area of the helmet base. Take a moderate latitudinal width of 15° for the helmet base and 0.5 $R_\odot$ for the length of the helmet belt that erupts into a CME. This area of the helmet base spans about 1% of the total solar surface. It follows that it would take 10,000 CMEs to remove the magnetic flux across the solar surface at any one time. Averaged over an 11-year solar cycle, the 10,000 CMEs gives a mean rate of 2.5 events a day, which is in the range of observed CME rates. If the helmet width is taken to be 30°, which is not unreasonable [*Hundhausen*, 1993], the calculated mean CME rate would drop to about 1.2 events a day.

Therefore the CMEs occuring during an 11-year cycle are capable of removing the magnetic flux across the photosphere at any one time. Being taken out along with the flux rope is the accumulated magnetic helicity. This exercise is, of course, not proof that such a flux transport actually takes place. Proof must come from unambiguous observation of this process. The exercise merely makes the persuasive point that with an amount as modest as 1% of the flux threading across the base of its helmet taken out by each CME, the effect is significant for the flux budgets in the photosphere and the corona. A different and more optimistic argument for this conclusion is given by *Bieber and Rust* [1995]. If this conclusion is valid, CMEs may be the fundamental process that systematically removes old flux from the corona to make room for the newly emerged flux of a new cycle. Furthermore, it implies that the dynamo in the solar interior suffers a significant leakage of magnetic flux into interplanetary space, an effect not traditionally considered in dynamo theories.

6. Conclusion

The synthesis of physical relationships among coronal phenomena we have presented came out of the hydromagnetic issues posed by observations. The consistency of the synthesis and its ability to connect the corona to the photosphere and the solar dynamo in specific physical terms suggest that we are perhaps posing the right physical questions. To conclude, we address a few observational and theoretical points important for future developments.

Observation, as always, holds the key to the main predictions of this synthesis, among which we take note of the following four: (1) The emergence of magnetic flux at the photosphere involves transport of a significant part of magnetic-flux systems into the corona. (2) The cavity in the coronal helmet is a magnetic flux rope of helical fields. (3) Some form of magnetic-helicity conservation constrains the liberation of magnetic free energy in flares. (4) The mass of prominences may play a significant role in anchoring the cavity magnetic flux rope. Observational tests of these predictions will have much to teach us. Most pressing is the need to directly observe the magnetic field in the corona outside of prominences [*Gary and Hurford*, 1994; *Kuhn et al.*, 1996; *Judge*, 1998].

Our synthesis provides motivation for theoretical calculations to show if the various hydromagnetic processes described are supported quantitatively in terms of basic principles. The hydromagnetic equilibrium of the helmet streamer deserves central attention, in terms of whether its internal structure does or does not contain the complexity of a cavity magnetic flux rope and a heavy prominence. This structure should also be investigated in terms of the hydromagnetic solar wind flowing in the external open-field regions. The fundamental questions to address are how and when magnetic-field confinement in the open atmosphere is possible and when that confinement may fail. This is a theoretical problem beset with nonlinearity and technical

challenges for numerical modelers. Progress in understanding this structure is crucial to a theory of CME origin and initiation such as described in this article and in many related or alternative theories cited in this review. Finally, the CME expulsion itself presents the basic problem of time-dependent hydromagnetic flow of a special kind, as described in section 2.

Numerical solutions that take the CME flow from the low-β corona out into the high-β interplanetary solar wind carry much nonlinear physics which we have only begun to explore. We are still a long way from understanding the fate of CMEs in interplanetary space, but many fundamental discoveries of that fate have been made in satellite observations [e.g., *Burlaga et al.*, 1994; *Burlaga et al.*, 1998; *Gosling*, 1993b; *Chen*, 1996; *Kumar and Rust*, 1996; *Gopalswamy et al.*, 1998; *Wu et al.*, 1999]. Developments in these different issues and others not mentioned for want of space in this article are timely for quantitative treatment. We will learn interesting physics which in turn will shed light on solar observations. This is an important step to a physical understanding of the coupled systems from the Sun through interplanetary space out to Earth orbit and beyond.

Acknowledgments. I thank Bryan Fong for reviewing this article, Alice Lecinski for preparing Figure 1, Joan Burkepile and Andy Stanger for preparing Plate 1, and Loren Acton for providing Figure 7. The 1980 eclipse photograph in Figure 1 came from a joint expedition of the High Altitude Observatory and Rhodes College. This work is supported in part under NASA grant W-19,323. The National Center for Atmospheric Research is sponsored by the National Science Foundation.

Janet G. Luhmann thanks David F. Webb and another referee for their assistance in evaluating this paper.

References

Aly, J. J., The properties of force-free magnetic fields in infinite regions of space, *Astrophys. J., 283*, 349, 1984.

Aly, J. J., How much energy can be stored in a three-dimensional force-free magnetic field?, *Astrophys. J., 375*, L61, 1991.

Aly, J. J., Nonequilibrium in sheared axisymmetric force-free magnetic fields, *Astrophys. J., 439*, L63, 1995.

Amari, T., J. F. Luciani, Z. Mikic, and J. Linker, Three-dimensional solutions of MHD equations for prominence magnetic support: Twisted magnetic flux rope, *Astrophys. J., 518*, L57, 1999.

Antiochos, S., The magnetic topology of solar eruptions, *Astrophys. J., 502*, L181, 1998.

Antiochos, S. K., R. B. Dahlburg, and J. A. Klimchuk, The magnetic field of solar prominences, *Astrophys. J., 420*, L41, 1991.

Antiochos, S. K., C. R. DeVore, and J. A. Klimchuk, A model of solar mass ejections, *Astrophys. J., 510*, 485, 1999.

Athay, R. G., The origin of spicules, *Sol. Phys.*, in press, 2001.

Athay, R. G., B. C. Low, and B. Rompolt, Characteristics of the expansion associated with eruptive prominences, *Sol. Phys., 110*, 359, 1987.

Aulanier, G., and P. Demoulin, 3D magnetic configurations supporting prominences, I, The natural presence of lateral feet, *Astron. Astrophys., 329*, 1125, 1998.

Bao, S., and H. Zhang, Patterns of current helicity for the 22nd solar cycle, *Astrophys. J., 496*, L43, 1998.

Berger, M. A., Rigorous new limits on magnetic helicity dissipation in the corona, *Geophys. Astrophys. Fluid Dyn., 30*, 79, 1984.

Berger, M. A., Magnetic helicity in space physics, in *Magnetic Helicity in Space and Laboratory Plasmas, Geophys. Monogr. Ser.*, vol. 111, edited by M. R. Brown, R. Canfield, and A. Petsov, pp. 1-9, AGU, Washington, D. C., 1999.

Berger, M. A., and G. B. Field, The topological properties of magnetic helicity, *J. Fluid Mech., 147*, 133, 1984.

Bieber, J. W., and D. M. Rust, The escape of magnetic flux from the Sun, *Astrophys. J., 453*, 911, 1995.

Burkepile, J. T., and O. C. St. Cyr, A revised and expanded catalogue of coronal mass ejections observed by the Solar Maximum Mission coronagraph, *Tech. Note TN-369+STR*, pp. 233, Natl. Cent. for Atmos. Res., Boulder, 1993.

Burlaga, L. F., L. W. Klein, N. R. Sheeley Jr., D. J. Michels, R. A. Howard, M. J. Koomen, R. Schwenn, and H. Rosenbauer, A magnetic cloud and a coronal mass ejection, *Sol. Phys., 155*, 69, 1994.

Burlaga, L., et al., A magnetic cloud containing prominence material: January 1997, *J. Geophys. Res., 103*, 277, 1998.

Canfield, R. C., H. S. Hudson, and D. E. McKenzie, Sigmoidal morphology and eruptive solar activity, *Geophys. Res. Lett., 26*, 627, 1999.

Chandrasekhar, S., *Hydrodynamic and Hydromagnetic Stability*, Oxford Univ. Press, New York, 1961.

Chen, J., Effects of toroidal forces in current loops embedded in a background plasma, *Astrophys. J., 338*, 453, 1989.

Chen, J., Theory of prominence eruption and propagation: Interplanetary consequences, *J. Geophys. Res., 101*, 27,499, 1996.

Chen, J., et al., Evidence of an erupting flux rope: LASCO coronal mass ejection of 1997 April 13, *Astrophys. J., 490*, L191, 1997.

Choe, G. S., and L. C. Lee, Formation of solar prominences by photospheric shearing motion, *Sol. Phys., 138*, 291, 1992.

Ciaravella, A., et al., SOHO observations of a helical coronal mass ejection, *Astrophys. J., 529*, 575, 2000.

Crooker, N., J.-A. Joselyn, and J. Feynman (Eds.), *Coronal Mass Ejections, Geophys. Monogr. Ser.*, vol. 99, 299 pp., AGU, Washington, D. C., 1997.

Dere, K. P., G. E. Brueckner, R. A. Howard, D. J. Michels, and J. P. Delaboudiniere, LASCO and EIT observations of helical structure in coronal mass ejections, *Astrophys. J., 516*, 465, 1999.

De Sterck, H., B. C. Low, and S. Poedts, Complex magneto-hydrodynamic bow shock topology in field-aligned low-β flow around a perfectly conducting cylinder, *Phys. Plasmas, 5*, 4015, 1998.

Donea, A. C., D. C. Braun, and C. Linsey, Seismic images of a solar flare, *Astrophys. J., 513*, L143, 1999.

Emonet, T., and F. Moreno-Insertis, The physics of twisted magnetic tubes rising in a stratified medium: Two-dimensional results, *Astrophys. J., 492*, 804, 1998.

Fan, Y., E. G. Zweibel, M. G. Linton, and G. H. Fisher, The rise of kink-unstable magnetic flux tubes and the origin of δ-configuration sunspot, *Astrophys. J., 521*, 460, 1999.

Feynman, J., and A. J. Hundhausen, Coronal mass ejections and major solar flares: The great active center of March 1989, *J. Geophys. Res., 99*, 8451, 1994.

Feynman, J., and S. F. Martin, The initiation of coronal

mass ejections by newly emerging magnetic flux, *J. Geophys. Res., 100*, 3355, 1995.

Fisher, R. R., Coronal mass ejection events, *Adv. Space Res., 4*, 163, 1984.

Fisher, R., and C. Garcia, Detection of a slowly moving coronal transient, *Astrophys. J., 282*, L35, 1984.

Fisher, R. R., and A. I. Poland, Coronal activity below 2 solar radii, *Astrophys. J., 246*, 1004, 1981.

Fong, B. H. L., Metastable and explosive properties of ballooning modes in laboratory and space plasmas, Ph.D. thesis, Princeton Univ., Princeton, N. J., 1999.

Forbes, T. G., A review on the genesis of coronal mass ejections, *J. Geophys. Res.*, 105, 23153, 2000.

Forbes, T. G., and P. A. Isenberg, A catastrophic mechanism for coronal mass ejections, *Astrophys. J., 373*, 294, 1991.

Fox, N. J., M. Peredo, and B. J. Thompson, Cradle to grave tracking of the January 6-11, 1997, Sun-Earth connection event, *Geophys. Res. Lett., 25*, 2461, 1998.

Gary, D. E., and G. J. Hurford, Coronal temperature, density, and magnetic field maps of a solar active region, *Astrophys. J., 420*, 903, 1994.

Gibson, S. E., and B. C. Low, A time-dependent, three-dimensional, magnetohydrodynamic model of the coronal mass ejection, *Astrophys. J., 493*, 460, 1998.

Gibson, S. E., and B. C. Low, Three-dimensional and twisted: An MHD interpretation of on-disk observational characteristics of coronal mass ejections, *J. Geophys. Res.*, 105, 18,187, 2000.

Gilbert, H., T. E. Holzer, J. T. Burkepile, and A. J. Hundhausen, Active and eruptive prominences and their relationship to coronal mass ejections, *Astrophys. J.*, 537, 503, 2000.

Golub, L., R. Rosner, G. S. Vaiana, and N. O. Weiss, Solar magnetic fields: The generation of emerging flux, *Astrophys. J., 243*, 309, 1981.

Gopalswamy, N., and Y. Hanaoka, Coronal dimming associated with a giant prominence eruption, *Astrophys. J., 498*, L179, 1998.

Gopalswamy, N., et al., On the relationship between coronal mass ejections and magnetic clouds, *Geophys. Res. Lett., 25*, 2485, 1998.

Gosling, J. T., The solar flare myth, *Geophys. Res. Lett., 98*, 18,937, 1993a.

Gosling, J. T., Coronal mass ejections: The link between solar and geomagnetic activity, *Phys. Fluids, 5*, 2638, 1993b.

Gosling, J. T., The role of reconnection in the formation of flux ropes in the solar wind, in *Magnetic Helicity in Space and Laboratory Plasmas*, edited by M. R. Brown, R. Canfield, and A. Pevtsov, pp. 205-212, AGU, Washington, D. C., 1999.

Gosling, J. T., E. Hildner, R. M. MacQueen, R. H. Munro, A. I. Poland, and C. L. Ross, Mass ejections from the Sun: A view from Skylab, *J. Geophys. Res., 79*, 4581, 1974.

Gosling, J. T., E. Hildner, R. M. MacQueen, R. H. Munro, A. I. Poland, and C. L. Ross, The speeds of coronal mass ejection events, *Sol. Phys., 48*, 389, 1976.

Guo, W. P., and S. T. Wu, A magnetohydrodynamic description of a coronal helmet streamer containing a cavity, *Astrophys. J., 494*, 419, 1998.

Harrison, R. A., Solar coronal mass ejections and flares, *Astron. Astrophys., 162*, 283, 1986.

Harvey, K. L., and V. Gaizauskas, Filament channels: Contrasting their structures in H_α and HeI 1083nm, in *New Perspectives on Solar Prominences*, edited by D. Webb, D. M. Rust, and B. Schmieder, *Astron. Soc. of the Pacific*, San Francisco, Calif., pp. 269-273, 1998.

Heyvaerts, J., and E. R. Priest, Coronal heating by reconnection in DC current systems, a theory based on Taylor's hypothesis, *Astron. Astrophys., 137*, 63, 1984.

Hiei, E., A. J. Hundhausen, and D. G. Sime, Reformation of a coronal helmet streamer by magnetic reconnection after a coronal mass ejection, *Geophys. Res. Lett., 20*, 2785, 1993.

Hirayama, T., Theoretical models of flares and prominences, *Sol. Phys., 34*, 323, 1974.

Howard, R. A., D. J. Michels, N. R. Sheeley Jr., and M. J. Koomen, The observation of a coronal transient directed at Earth, *Astrophys. J., 263*, L101, 1982.

Howard, R. A., N. R. Sheeley Jr., M. J. Koomen, and D. J. Michels, Coronal mass ejections: 1979-1981, *J. Geophys. Res., 90*, 8173, 1985.

Howard, R. A., et al., Observations of CMEs from SOHO/LASCO, in *Coronal Mass Ejections, Geophys. Monogr. Ser.*, vol. 99, edited by N. Crooker, J. A. Joselyn, and J. Feynman, pp. 17-26, AGU, Washington D. C., 1997.

Hu, Y. Q., Z. W. Zhu, A. J. Hundhausen, T. E. Holzer, and B. C. Low, Slow shocks in open magnetic fields near the Sun, *Sci. China, 33*, 332, 1990.

Hudson, H., B. Haisch, and K. T. Strong, Comment on "The solar flare myth" by J. T. Gosling, *J. Geophys. Res., 100*, 3473, 1995.

Hudson, H. S., L. W. Acton, K. L. Harvey, and D. E. McKenzie, A stable filament cavity with a hot core, *Astrophys. J., 513*, L83, 1999.

Hundhausen, A. J., *Coronal Expansion and Solar Wind*, Springer-Verlag, New York, 1972.

Hundhausen, A. J., The origin and propagation of coronal mass ejections, in *Solar Wind Six*, edited by V. Pizzo, D. G. Sime, and T. E. Holzer, *Tech. Note NCAR/TN-306+Proc.*, Natl. Cent. for Atmos. Res., Boulder, Colo., pp. 181-214, 1987.

Hundhausen, A. J., Sizes and locations of coronal mass ejections: SMM observations from 1980 and 1984-1989, *J. Geophys. Res., 98*, 13,177, 1993.

Hundhausen, A. J., Coronal diagnostics (and some dynamics), in *Solar System Plasma Physics*, edited by F. Mariani and N. F. Ness, pp. 21-42, Editrice Comp., Bologna, Italy, 1997.

Hundhausen, A. J., Coronal mass ejections: A summary of SMM observations from 1980 and 1984-1989, in *The Many Faces of the Sun*, edited by K. Strong et al., pp. 143-200, Springer-Verlag, New York, 1999.

Hundhausen, A. J., J. T. Burkepile and O. C. St. Cyr, Speeds of coronal mass ejections: SMM observations from 1980 and 1984-1989, *J. Geophys. Res., 99*, 6543, 1994.

Hundhausen, A. J., T. E. Holzer, and B. C. Low, Do slow shocks precede some coronal mass ejections, *J. Geophys. Res., 92*, 11,173, 1987.

Illing, R. M. E., The complex coronal transient of 1980 March 23, *Astrophys. J., 280*, 399, 1984.

Illing, R. M. E., and A. J. Hundhausen, Possible observation of a disconnected magnetic structure in a coronal transient, *J. Geophys. Res., 88*, 10,210, 1983.

Illing, R. M. E., and A. J. Hundhausen, Observation of a coronal transient from 1.2 to 6 solar radii, *J. Geophys. Res., 90*, 275, 1985.

Illing, R. M. E., and A. J. Hundhausen, Disruption of a coronal streamer by an eruptive prominence and coronal mass ejection, *J. Geophys. Res., 91*, 10,951, 1986.

Isenberg, P. A., T. G. Forbes, and P. Demoulin, Catastrophic evolution of a force-free flux rope: A model for eruptive flares, *Astrophys. J., 417*, 368, 1993.

Ishii, T. T., H. Kurokawa, and T. T. Takeuchi, Emergence of a twisted magnetic flux bundle as a source of strong flare activity, *Astrophys. J., 499*, 898, 1998.

Judge, P. G., Spectral lines for polarization measurements of the coronal magnetic field, I, Theoretical intensities, *Astrophys. J., 500*, 1009, 1998.

Judge, P. G., V. Hansteen, O. Wikstol, and T. Moran, Ev-

idence in support of the "nanoflare" picture of coronal heating from SUMER data, *Astrophys. J., 502*, 981, 1998.
Kahler, S. W., Solar flares and coronal mass ejections, *Annu. Rev. Astron. Astrophys., 30*, 113, 1992.
Kopp, R. A., and G. W. Pneuman, Magnetic reconnection in the corona and the loop prominence phenomenon, *Sol. Phys., 50*, 85, 1976.
Kuhn, J. R., M. J. Penn, and J. Mann, The near-infrared coronal spectrum, *Astrophys. J., 456*, L67, 1996.
Kulsrud, R. M., Magnetic reconnection in a magnetohydrodynamic plasma, *Phys. Plasmas, 5*, 1599, 1998.
Kumar, A., and D. M. Rust, Interplanetary magnetic clouds, helicity conservation, and current-core flux-ropes, *J. Geophys. Res., 101*, 15,667, 1996.
Kurokawa, H., Two distinct morphological types of magnetic shear development and their relation to flares, *Sol. Phys., 113*, 259, 1987.
Leka, K. D., R. C. Canfield, A. N. McClymont, and L. van Driel-Gesztelyi, Evidence for current-carrying emerging flux, *Astrophys. J., 462*, 547, 1996.
Leroy, J. L., Observation of prominence magnetic fields, in *Dynamics and Structures of Quiescent Prominences*, edited by E. R. Priest, pp. 77-113, Kluwer Acad., Norwell, Mass., 1989.
Li, J., J. C. Raymond, L. W. Acton, J. L. Kohl, M. Romoli, G. Noci, and G. Naletto, Physical structure of a coronal streamer in the closed-field region as observed from UVCS/SOHO and SXT/Yohkoh, *Astrophys. J., 506*, 431, 1998.
Lin, J., T. G. Forbes, P. A. Isenberg, and P. Demoulin, The effect of curvature on flux-rope models of coronal mass ejections, *Astrophys. J., 504*, 1006, 1998.
Linker, J., and Z. Mikic, Disruption of a helmet-streamer by photospheric shear, *Astrophys. J., 438*, L45, 1995.
Linton, M. G., R. B. Dahlburg, G. H. Fisher, and D. W. Longcope, Nonlinear evolution of kink unstable magnetic flux tube and solar δ-spot active regions, *Astrophys. J., 507*, 404, 1998.
Lionello, R., M. Velli, G. Einaudi, and Z. Mikic, Nonlinear magnetohydrodynamic evolution of line-tied coronal loops, *Astrophys. J., 498*, 840, 1998.
Lipscy, S., A research program exploring the relationship between coronal mass ejections and erupting prominences, honors thesis, Univ. of Colo., Boulder, Colo., 1998.
Lites, B. W., and B. C. Low, Flux emergence and prominences: A new scenario for 3-dimensional field geometry based on observations with the Advanced Stokes Polarimeter, *Sol. Phys., 174*, 91, 1997.
Lites, B. W., B. C. Low, V. Martinez-Pillet, P. Seagraves, A. Skumanich, Z. A. Frank, R. A. Shine, and S. Tsuneta, The possible ascent of a closed magnetic system through the photosphere, *Astrophys. J., 446*, 877, 1995.
Longbottom, A. W., G. J. Rickard, I. J. D. Craig, and A. D. Sneyd, Magnetic flux braiding: Force-free equilibria and current sheets, *Astrophys. J., 500*, 471, 1998.
Low, B. C., Evolving force-free magnetic fields, I, The development of the preflare stage, *Astrophys. J., 212*, 234, 1977.
Low, B. C., Eruptive solar magnetic fields, *Astrophys. J., 251*, 352, 1981.
Low, B. C., Self-similar magnetohydrodynamics, I, The $\gamma = 4/3$ polytrope and the coronal transient, *Astrophys. J., 254*, 796, 1982.
Low, B. C., Self-similar magnetohydrodynamics, IV, The physics of coronal transients, *Astrophys. J., 281*, 392, 1984.
Low, B. C., Blow-up of force-free magnetic field in the infinite region of space, *Astrophys. J., 310*, 953, 1986.
Low, B. C., Equilibrium and dynamics of coronal magnetic fields, *Annu. Rev. Astron. Astrophys., 28*, 491, 1990.
Low, B. C., Three dimensional structures of magnetostatic atmospheres, IV, Magnetic structures over solar active regions, *Astrophys. J., 399*, 300, 1992.
Low, B. C., Mass acceleration processes: The case of coronal mass ejections, *Adv. Space Res., 13*, 63, 1993a.
Low, B. C., Force-free magnetic fields with singular current-density surface, *Astrophys. J., 409*, 798, 1993b.
Low, B. C., Magnetohydrodynamic processes in the solar corona: Flares, coronal mass ejections, and magnetic helicity, *Phys. Plasmas, 1*, 1684, 1994.
Low, B. C., Solar activity and the corona, *Sol. Phys., 167*, 217, 1996.
Low, B. C., The role of coronal mass ejections in solar activity, in *Coronal Mass Ejections, Geophys. Monogr. Ser.*, vol. 99, edited by N. Crooker, J. Joselyn, and J. Feynman, pp. 39-47, AGU, Washington, D. C., 1997.
Low, B. C. Coronal mass ejections, flares, and prominences, in *Solar Wind Nine*, edited by S. R. Habbal et al., *AIP Conf. Proc., 471*, 109, 1999a.
Low, B. C., Magnetic energy and helicity in open systems, in *Magnetic Helicity in Space and Laboratory Plasmas, Geophys. Monogr. Ser.*, vol. 111, edited by M. R. Brown, R. Canfield, and A. Pevtsov, pp. 25-32, AGU, Washington, D. C., 1999b.
Low, B. C., and A. J. Hundhausen, The velocity field of a coronal mass ejection: The event of September 1, 1980, *J. Geophys. Res., 92*, 2221, 1987.
Low, B. C. and J. R. Hundhausen, Magnetostatic structures of the solar corona, II, The magnetic topology of quiescent prominences, *Astrophys. J., 443*, 818, 1995.
Low, B. C., and D. F. Smith, The free energies of partially open coronal magnetic fields, *Astrophys. J., 410*, 413, 1993.
Low, B. C., R. H. Munro, and R. R. Fisher, The initiation of a coronal transient, *Astrophys. J., 254*, 335, 1982.
Luhmann, J. G., J. T. Gosling, J. T. Hoeksema, and X. Zhao, The relationship between large-scale solar magnetic field evolution and coronal mass ejections, *J. Geophys. Res., 103*, 6585, 1998.
MacQueen, R. M., Coronal transients: A summary, *Philos. Trans. R. Soc. London, Ser. A, 297*, 605, 1980.
MacQueen, R. M., and R. R. Fisher, The kinematics of solar inner coronal transients, *Sol. Phys., 89*, 89, 1983.
MacQueen, R. M., J. T. Burkepile, T. E. Holzer, A. L. Stanger, and K. E. Spence, Solar coronal brightness changes and mass ejections during solar cycle 22, *Astrophys. J., 549*, 1175, 2001.
Manchester, W., IV, The equilibria, stability and nonlinear dynamics of magnetically-sheared atmospheres with applications to the solar environment, Ph.D. thesis, Univ. of Ill., Urbana, 2000.
Martin, S. F., R. Bilimoria, and P. W. Tracados, Magnetic field configurations basic to filament channels and filaments, in *Solar Surface Magnetism*, edited by R. J. Rutten and C. J. Schrijver, pp. 303-338, Kluwer Acad., Norwell, Mass., 1994.
Mason, S. F., and R. J. Bessey, The formation of prominences by thermal instability: A numerical study, *Sol. Phys., 83*, 121, 1983.
Mikic, Z., and J. Linker, Disruption of coronal magnetic field arcades, *Astrophys. J., 430*, 398, 1994.
Moffatt, H. K., *Magnetic Field Generation in Electrically Conducting Fluids*, Cambridge Univ. Press, New York, 1978.
Montgomery, D. C., and J. W. Bates, Helicity and its role in the varieties of magnetohydrodynamic turbulence, in *Magnetic Helicity in Space and Laboratory Plasmas, Geophys. Monogr. Ser.*, vol. 111, edited by M. R. Brown, R. Canfield, and A. Pevtsov, pp. 33-46, AGU, Washington, D. C., 1999.

Niita, N., and S. Akiyama, Relationship between flare-associated X-ray ejections and coronal mass ejections, *Astrophys. J., 525*, L57, 1999.

Ohyama, M., and K. Shibata, X-ray plasma ejection associated with an impulsive flare on 1992 October 5: Physical conditions of X-ray plasma ejection, *Astrophys. J., 499*, 934, 1998.

Parker, E. N., *Interplanetary Dynamical Processes*, Wiley-Interscience, New York, 1963.

Parker, E. N., *Cosmical Magnetic Fields*, Oxford Univ. Press, New York, 1979.

Parker, E. N., *Spontaneous Current Sheets in Magnetic Fields*, Oxford Univ. Press, New York, 1994.

Pevtsov, A. A., and R. C. Canfield, Helicity of photospheric magnetic fields, in *Magnetic Helicity in Space and Laboratory Plasmas, Geophys. Monogr. Ser.*, vol. 111, edited by M. R. Brown, R. C. Canfield, and A. A. Pevtsov, pp. 103-110, AGU, Washington, D. C., 1999.

Plunkett, S. P., B. J. Thompson, R. A. Howard, D. J. Michels, O. C. St. Cyr, S. J. Tappin, R. Schwenn, and P. L. Lamy, LASCO observation of an Earth-directed coronal mass ejection on May 12, 1997, *Geophys. Res. Lett., 25*, 2477, 1998.

Poland, A. I., and R. M. MacQueen The evolution of a coronal streamer and the photospheric magnetic field, *Sol. Phys., 71*, 361, 1981.

Priest, E. R., *Solar Magnetohydrodynamics*, D. Reidel, Norwell, Mass., 1982.

Priest, E. R., A. W. Hood, and U. Anzer, A twisted flux-tube model for solar prominences, I, General properties, *Astrophys. J., 344*, 1010, 1989.

Richardson, R. S., The nature of solar hydrogen vortices, *Astrophys. J., 93*, 24, 1941.

Rusin, V., and M. Rybansky, Eruptive prominence of August 16, 1980, *Bull. Astron. Inst. Czech., 33*, 219, 1982.

Rust, D. M., Spawning and shedding helical fields in the solar atmosphere, *Geophys. Res. Lett., 21*, 241, 1994.

Rust, D. M., and A. Kumar, Helical magnetic fields in filaments, *Sol. Phys., 155*, 69, 1994.

Rust, D. M., and A. Kumar, Evidence for helically kinked magnetic flux ropes in solar eruptions, *Astrophys. J., 464*, L199, 1996.

Ruzmaikin, A., and P. Akhmetiev, Topological invariants of magnetic fields, and the effect of reconnection, *Phys. Plasmas, 1*, 331, 1994.

Schonfelder, A. O., and A. Hood, Current sheet models for inverse polarity prominences in twisted flux tubes, *Sol. Phys., 157*, 223, 1995.

Seehafer, N., Electric current helicity in the solar atmosphere, *Sol. Phys., 125*, 219, 1990.

Serio, S., G. S. Vaiana, G. Godoli, V. Pirronello, and R. A. Zappaloa, Configuration and gradual dynamics of prominence related X-ray coronal cavities, *Sol. Phys., 59*, 65, 1978.

Sheeley, N. R., Jr., R. A. Howard, M. J. Koomen, D. J. Michels, R. Schwenn, K. H. Muhlhauser, and H. Rosenhauer, Coronal mass ejections and interplanetary shocks, *J. Geophys. Res., 90*, 163, 1985.

Sheeley, N. R., Jr., J. H. Walters, Y. M. Wang, and R. A. Howard, Continuous tracking of coronal outflows: Two kinds of coronal mass ejections, *J. Geophys. Res., 104*, 24,739, 1999.

Shibata, K., Evidence of magnetic reconnection in solar flares and a unified model of flares, *Astrophys. Space Sci.*, 264, 129-144, 1999.

Sime, D. G., and J. Streete, Solar coronal structure near the time of the 1991 July 11 total solar eclipse, *Astrophys. J., 408*, 368, 1993.

Sime, D. G., R. R. Fisher, and D. L. Mickey, Solar coronal and magnetic field observations near the time of the 1988 March 18 solar eclipse, *Astrophys. J., 333*, L103, 1988.

Smith, E. A., and E. R. Priest, The formation of solar prominences by thermal instability in a current-sheet, *Sol. Phys., 53*, 25, 1977.

Spruit, H. C., A. M. Title, and A. A. van Ballegooijen, Is there a weak mixed polarity background field? Theoretical argument, *Sol. Phys., 110*, 115, 1987.

Srivastava, N., R. Schwenn, B. Inhester, G. Stenborg, and B. Podlipnik, Measurements of flow speeds and acceleration in gradually evolving solar mass ejections as observed by LASCO, in *Solar Wind Nine*, edited by S. R. Habbal et al., *AIP Conf. Proc., 471*, 115, 1999.

St. Cyr, O. C., J. T. Burkepile, A. J. Hundhausen, and A. R. Lecinski, A comparison of ground-based and spacecraft observations of coronal mass ejections from 1980-1989, *J. Geophys. Res., 104*, 12,493, 1999.

St. Cyr, O. C., et al., Properties of coronal mass ejections: SOHO LASCO observations from January 1996 to June 1998, *J. Geophys. Res., 105*, 18,169, 2000.

St. Cyr, O. C., R. A. Howard, N. R. Sheeley. Jr., S. P. Plunkett, D. J. Michels, S. E. Paswaters, M. J. Koomen, G. M. Simnett, B. J. Thompson, J. B. Gurman, R. Schwenn, D. F. Webb, E. Hildner, and P. L. Lamy, Properties of coronal mass ejections: SOHO LASCO observations from January 1996 to June 1998, *J. Geophys. Res., 105*, 18169, 2000.

Steinolfson, R. S., Coronal evolution due to shear motion, *Astrophys. J., 382*, 677, 1991.

Steinolfson, R. S., and A. J. Hundhausen, MHD intermediate shocks in coronal mass ejections, *J. Geophys. Res., 95*, 6389, 1990.

Sterling, A. C., and H. Hudson, Yohkoh SXT observations of X-ray dimming associated with a halo coronal mass ejection, *Astrophys. J., 491*, L55, 1997.

Sterling, A. C., H. S. Hudson, B. J. Thompson, and D. M. Zarro, Yohkoh SXT and SOHO EIT observations of sigmoid-to-arcade evolution of structures associated with halo coronal mass ejections, *Astrophys. J., 532*, 628, 2000.

Sturrock, P. A., Maximum energy of semi-infinite magnetic configurations, *Astrophys. J., 380*, 655, 1991.

Tandberg-Hanssen, E., *Solar Prominences*, D. Reidel, Norwell, Mass., 1974.

Tandberg-Hanssen, E., *The Nature of Solar Prominences*, Kluwer Acad., Norwell, Mass., 1995.

Taylor, J. B., Relaxation and magnetic reconnection in plasmas, *Rev. Mod. Phys., 58*, 741, 1986.

Thompson, B. J., S. P. Plunkett, J. B. Gurman, J. S. Newmark, O. C. St. Cyr, and D. J. Michels, SOHO/EIT observations of an Earth-directed coronal mass ejection on May 12, 1997, *Geophys. Res. Lett., 25*, 2465, 1998.

Tsuneta, S., Moving plasmoid and the formation of the neutral sheet in a solar flare, *Astrophys. J., 483*, 507, 1997.

van Ballegooijen, A. A., and P. C. H. Martens, Formation and eruption of solar prominences, *Astrophys. J., 343*, 971, 1989.

van Ballegooijen, A. A., and P. C. H. Martens, Magnetic fields in quiescent prominences, *Astrophys. J., 361*, 283, 1990.

Vrsnak, B., Prominence eruptions, in *New Perspectives on Solar Prominences*, edited by D. Webb, D. M. Rust, and B. Schmieder, pp. 302-309, *Astron. Soc. of the Pacific*, San Francisco, Calif., 1998.

Vrsnak, B., V. Ruzdjak, and B. Rompolt, Stability of prominences exposing helical-like patterns, *Sol. Phys., 136*, 151, 1991.

Webb, D. F., Erupting prominences and the geometry of coronal mass ejections, *J. Geophys. Res., 93*, 1749, 1988.

Webb, D. F., and E. W. Cliver, Evidence for magnetic dis-

connection of mass ejections in the corona, *J. Geophys. Res., 100*, 5853, 1995.

Webb, D. F., and R. A. Howard, The solar cycle variation of coronal mass ejections and the solar-wind mass flux, *J. Geophys. Res., 99*, 4201, 1994.

Webb, D. F., S. W. Kahler, P. S. McIntosh, and J. A. Klimchuk, Large-scale structures and multiple neutral lines associated with coronal mass ejections, *J. Geophys. Res., 102*, 24,161, 1997.

Wolfson, R., Energy requirements for opening up the solar corona, *Astrophys. J., 419*, 382, 1993.

Wolfson, R., and B. Dlamini, Cross-field currents: An energy source for coronal mass ejections, *Astrophys. J., 483*, 961, 1997.

Wolfson, R., and B. Dlamini, Magnetic shear and cross-field currents: Roles in the evolution of the pre-coronal mass ejection corona, *Astrophys. J., 526*, 1046, 1999.

Wolfson, R., and B. C. Low, Energy build-up in sheared force-free magnetic fields, *Astrophys. J., 391*, 353, 1992.

Wolfson, R., and S. Saran, Energetics of coronal mass ejections: Role of the streamer cavity, *Astrophys. J., 499*, 496, 1998.

Wood, B. E., M. Larovska, J. Chen, G. E. Bruekner, J. W. Cook, and R. A. Howard, Comparison of two coronal mass ejections observed by EIT and LASCO with a model of an erupting magnetic flux rope, *Astrophys. J., 512*, 484, 1999.

Wu, S. T., et al., MHD interpretation of LASCO observations of a coronal mass ejection as a disconnected magnetic structure, *Sol. Phys., 175*, 719, 1997

Wu, S. T., W. P. Guo, D. J. Michels, and L. F. Burlaga, MHD description of the dynamical relationships between a flux rope, streamer, coronal mass ejection, and magnetic cloud: An analysis of the January 1997 Sun-Earth connection event, *J. Geophys. Res., 104*, 14,789, 1999.

Zarro, D. M., A. C. Sterling, B. J. Thompson, H. S. Hudson, and N. Nitta, SOHO/EIT observations of EUV dimmings associated with a halo coronal mass ejection, *Astrophys. J., 520*, L139, 1999.

Zhang, H., and S. Bao, Distribution of photospheric electric current helicity and solar activities, *Astrophys. J., 519*, 876, 1999.

B. C. Low, High Altitude Observatory, National Center for Atmospheric Research, Boulder, Colorado, USA

(Received May 19, 2000; revised August 14, 2000; accepted August 14, 2000.)